Neurocomputing 149 (2015) 1370–1386

Contents lists available at ScienceDirect

Neurocomputing

journal homepage: www.elsevier.com/locate/neucom

Dynamical analysis and optimal control for a malware propagation model in an information network

Linhe Zhu, Hongyong Zhao *

Department of Mathematics, Nanjing University of Aeronautics and Astronautics, Nanjing 210016, China

ARTICLE INFO

Article history:
Received 30 June 2014
Accepted 29 August 2014
Communicated by H. Jiang
Available online 16 September 2014

Keywords:
Information networks
Stability
Hopf bifurcation
Malware propagation
Optimal control strategy

ABSTRACT

With the rapid development of network information technology, information networks security has become a very critical issue in our work and daily life. This paper investigates a nonlinear malware propagation model in wireless sensor networks (WSNs) based on SIR epidemic model. Sufficient conditions for the local stability of the positive equilibrium point and the existence of Hopf bifurcation are obtained by analyzing the associated characteristic equation. Moreover, formulas for determining the properties of the bifurcating periodic oscillations are derived by applying the normal form method and center manifold theorem. Furthermore, with the help of the Maximum Principle of Pontryagin, we design an optimal control strategy for the previous model to extend the region of stability and reduce the density of infected nodes in WSNs. Finally, we conduct extensive simulations to evaluate the proposed model. Numerical evidence shows that the dynamic characteristics of malware propagation in WSNs are closely related to the immune period of a recovered node and the rate constant for nodes becoming susceptible again after recovered. Besides, we obtain that the optimal control strategy effectively improves the performance of the networks.

© 2014 Elsevier B.V. All rights reserved.

1. Introduction

With the rapid development of the information and communication technology, information networks have become more prevalent in our work and daily life. Over the years, these information networks have been successfully used in hardware design, communication protocols, resource efficiency, home security, battlefield surveillance and other aspects [1–3]. Wireless sensor network, as a novel information and communication network, has gained worldwide attention in recent years [4–6]. In general, a WSN is composed of hundreds or even thousands of small, low cost, low power sensor nodes, which has facilitated the development of smart sensors. However, as WSNs are unfolding their vast potential in a plethora of application environment, information security has become one of the most critical challenges yet to be fully addressed. Because sensor nodes are resource constrained, they generally have weak defense capabilities and are attractive targets for software attacks (like malware attacks on the information networks). As malware being injected into some nodes in WSNs, the networks will fall out of stability and at the same time the oscillation by large amplitude occurring through Hopf bifurcation may appear, which possibly leads to that the utilization of the network decreases and the network performance declines. The oscillatory phenomena have been observed in many other similar networks, with rhythms originating from isolated components or emerging as a property of a network as a whole [7–9].

To defend against the malware propagation, we need to accurately understand the dynamic characteristics of malware propagation. In recent years, some analytical models have been brought into malware propagation system so that large strides have been taken in the research in WSNs [10–16]. The simulations and matching with practical data show that most of these models can not only describe the process of information and disease diffusion in human society, but also capture the process of malware propagation in computer networks such as the Internet and WSNs. In [13], the author proposed a percolation theory based evaluation of the spread of an epidemic on graphs with given degree distributions. However, [13] had payed little attention to the temporal dynamics of epidemic spread and only studied the final outcome of an infection spread. The authors in [14] proposed a spatial-temporal model for characterizing malware propagation in networks based on probabilistic graphs and spatial-temporal random processes. The basic idea was to abstract malware propagation into a probabilistic graph, and described the statistical dependence of malware propagation in arbitrary topologies using a spatial-temporal random process. Based on the ordinary differential equation and the SIR model, Wang in [15,16] derived the threshold for a piece of malware

* Corresponding author.
E-mail address: hongyongz@126.com (H. Zhao).

http://dx.doi.org/10.1016/j.neucom.2014.08.060
0925-2312/© 2014 Elsevier B.V. All rights reserved.

to propagate in WSNs, where all the nodes were supposed to be stationary. Furthermore, the author gave the sufficient conditions of stability and Hopf bifurcation of the malware propagation model.

As is well known, the periodic oscillation occurring through Hopf bifurcation in WSNs may destroy, block regular communications, or even damage the integrity of regular data packets. Thus, it is necessary to propose a control strategy to ensure that the system is stable and reliable operation. On the other hand, in order to reduce infected nodes in WSNs at minimal cost, in this paper we consider optimal control strategies associated with elimination policy and defense policy including execution costs based on the previous model. In fact, the optimal control theory [17], which was developed by Pontryagin and his co-workers in the late 1950s, has been applied to many areas including economics, management, engineering and biology [18–21]. In [22], Gumel and Moghadas proposed a model for the dynamics of an infectious disease in the presence of a preventive vaccine considering non-linear incidence rate and found the optimal vaccine coverage threshold needed for disease control and eradication. Swan [23] applied control theory to obtain maximal benefits interims of social benefits from the parsimonious use of insufficient public funds in the control of epidemics. With the help of the Maximum Principle of Pontryagin [24,25] and an iterative method we shall develop some new model with optimal control strategy. The goal of this work is not to consider a process of malware propagation but to present a method of how to treat this class of optimization problems. Our main contributions are summarized as follows.

(1) Through the analysis of the mechanism of malware propagation in WSNs, we generally quantify the process of malware propagation in WSNs based on the SIR model in the epidemic theory, and then we develop a delayed malware propagation model with logistic growth process. At the same time, we conduct extensive simulations on large-scale WSNs to evaluate the proposed model. Numerical evidence shows that the dynamic characteristics of malware propagation in WSNs are closely related to the immune period of a recovered node and the rate constant for nodes becoming susceptible again after recovered.
(2) Through the stability and Hopf bifurcation analysis of the positive equilibrium point for the proposed model, we obtain the sufficient conditions whether a series of oscillation phenomenon occurs through a Hopf bifurcation in WSNs. When the system occurs periodic oscillation, based on the normal form method and center manifold theorem we analysis the property of periodic oscillation.
(3) Based on our proposed model, with time increasing the distribution of infected nodes can be effectively predicted in advance. On this basis, the optimal control strategy we proposed can delay Hopf bifurcation and extend the stability region. Furthermore, we derive optimal state solutions associated with the optimal control variable $u^*(t)$ for the optimal control problem by means of the Pontryagin's Maximum Principle. Numerical results exhibit that the optimal control strategy ensures the security of WSNs and the regular communications between nodes. This will provide new insights on when and where countermeasures should be employed for preventing, controlling and removing malware propagation in WSNs.

The structure of this paper is arranged as follows. In Section 2, we consider the mechanism of malware propagation and the model formulation problem. In Section 3, we study the local stability and the existence of Hopf bifurcation. In Section 4, we give formula determining the direction of Hopf bifurcation and the stability of the bifurcating periodic solutions. In Section 5, we propose an optimal control strategy for malware propagation in WSNs. Finally, to support our theoretical predictions, some numerical simulations are given which support the analysis in Sections 3–5.

2. Model formulation

A WSN consists of many static and identical wireless sensors. Each wireless sensor is called a node. At any time, a node is classified as either *internal* or *external* accordingly as it is connected to the networks or not at that time. Generally, the nodes can be divided into three classes depending on their states: susceptible (healthy), infected and recovered (immunized). In this paper, we use $S(t)$, $I(t)$, $R(t)$ to denote the densities of susceptible nodes, infected nodes and recovered nodes at time t, respectively.

Based on the classical SIR epidemic model [26–28], we consider the following four facts:

(i) The susceptible nodes are assumed to have the logistic growth with carrying capacity K ($K>0$) as well as intrinsic increase rate constant r ($r>0$), and the incidence term is of bilinear mass action.
(ii) Users may immunize their nodes with countermeasures in state I.
(iii) Some recovered nodes go through a temporary immunity with probability δ.
(iv) As the energy of nodes is exhausted, more and more nodes become dead nodes. Any malware residing in other nodes cannot infect these dead nodes. Moreover, when a node dies, it becomes a dead node. All of the malware which ever resided in the dead nodes immediately disappear from the dead nodes. This means that the dead nodes no longer participate in the process of malware propagation in WSNs.

Our assumption on the dynamical transfer of the nodes is depicted in Fig. 1. As a result, the SIRS model can be formulated by the following delayed differential equations:

$$\begin{cases} \dfrac{dS}{dt} = rS\left(1-\frac{S}{K}\right) - \beta SI - \eta S + \delta R(t-\tau), \\ \dfrac{dI}{dt} = \beta SI - \varepsilon I - \eta I, \\ \dfrac{dR}{dt} = \varepsilon I - \eta R - \delta R(t-\tau), \end{cases} \tag{2.1}$$

with initial conditions

$$\begin{cases} S(t) = S_0 \geq 0, & t \in [-\tau, 0], \\ I(t) = I_0 \geq 0, & t \in [-\tau, 0], \\ R(t) = R_0 \geq 0, & t \in [-\tau, 0], \end{cases} \tag{2.2}$$

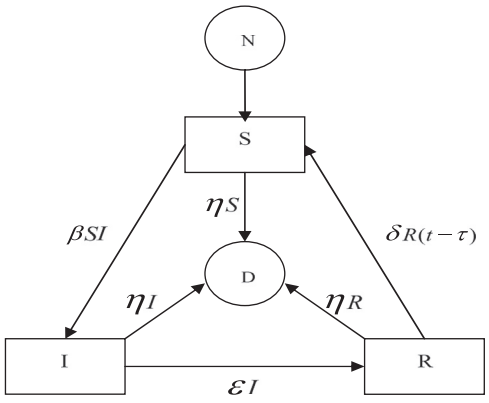

Fig. 1. Node state transition relationship, where N and D represent new nodes and death nodes, respectively.

where K, r, β, η, δ, ε are positive constants and τ is non-negative constant. The constant K is the carrying capacity the networks, r is the intrinsic increase rate, β is the constant contact rate between S and I, η is the death rate of nodes, δ is the rate constant for nodes becoming susceptible again after recovered, ε is the rate constant for nodes leaving the infective class I for recovered class R, τ is the immune period of a recovered node [29]. S_0, I_0 and R_0 are the initial density of susceptible nodes, infected nodes and recovered nodes, respectively.

3. Local stability and Hopf bifurcation

In this section, considering the delay τ as the bifurcation parameter, we will discuss the local stability and Hopf bifurcation of system (2.1) by analyzing the corresponding characteristic equation.

It can be seen that the zero equilibrium point always being the malware-free equilibrium point for any feasible parameters, $E^1=((K(r-\eta)/r),0,0)^T$ always being the boundary equilibrium point under the condition (H_1)

$$(H_1)\quad r-\eta>0,$$

and system (2.1) having a unique positive equilibrium point $E^*=(S^*,I^*,R^*)^T$ provided that the condition

$$(H_2)\quad r(K\beta-\varepsilon-\eta)-K\beta\eta>0$$

holds, where

$$S^*=\frac{\varepsilon+\eta}{\beta},\quad I^*=\frac{(\eta+\delta)(\eta+\varepsilon)[r(K\beta-\varepsilon-\eta)-K\beta\eta]}{K\eta\beta^2(\varepsilon+\eta+\delta)},$$
$$R^*=\frac{\varepsilon(\eta+\varepsilon)[r(K\beta-\varepsilon-\eta)-K\beta\eta]}{K\eta\beta^2(\varepsilon+\eta+\delta)}.$$

Under the condition (H_2), let $\tilde{S}=S-S^*$, $\tilde{I}=I-I^*$, $\tilde{R}=R-R^*$, and drop bars for the simplicity of notations. Then system (2.1) can be transformed into the following form:

$$\begin{cases}\dfrac{dS}{dt}=\left(r-\dfrac{2rS^*}{K}-\beta I^*-\eta\right)S-\beta S^*I+\delta R(t-\tau)-\beta SI-\dfrac{r}{K}S^2,\\ \dfrac{dI}{dt}=\beta I^*S+(\beta S^*-\eta-\varepsilon)I+\beta SI,\\ \dfrac{dR}{dt}=\varepsilon I-\eta R-\delta R(t-\tau).\end{cases}\tag{3.1}$$

Thus, the positive equilibrium point $E^*=(S^*,I^*,R^*)^T$ of system (2.1) is transformed into the zero equilibrium point $E_0=(0,0,0)^T$ of system (3.1). In the following, we will analysis stability and bifurcation of the zero equilibrium point E_0 of system (3.1).

The linearizing system of Eq. (3.1) at E_0 is

$$\begin{cases}\dfrac{dS}{dt}=\left(r-\dfrac{2rS^*}{K}-\beta I^*-\eta\right)S-\beta S^*I+\delta R(t-\tau),\\ \dfrac{dI}{dt}=\beta I^*S+(\beta S^*-\eta-\varepsilon)I,\\ \dfrac{dR}{dt}=\varepsilon I-\eta R-\delta R(t-\tau).\end{cases}\tag{3.2}$$

Then the corresponding characteristic equation of system (3.2) is

$$\begin{vmatrix}\lambda+\frac{2rS^*}{K}+\beta I^*+\eta-r & \beta S^* & -\delta e^{-\lambda\tau}\\ -\beta I^* & \lambda+\varepsilon+\eta-\beta S^* & 0\\ 0 & -\varepsilon & \lambda+\eta+\delta e^{-\lambda\tau}\end{vmatrix}=0.$$

That is

$$\lambda^3+\left(\frac{2rS^*}{K}+\beta I^*+2\eta-r\right)\lambda^2+\left[\eta\left(\frac{2rS^*}{K}+\beta I^*+\eta-r\right)+\beta^2S^*I^*\right]\lambda$$
$$+\beta^2\eta S^*I^*+\left[\lambda^2+\left(\frac{2rS^*}{K}+\beta I^*+\eta-r\right)\lambda+(\beta^2S^*I^*-\beta I^*\varepsilon)\right]\delta e^{-\lambda\tau}=0.\tag{3.3}$$

It is well know that the stability of the zero equilibrium point E_0 depends on the distribution of the characteristic root of (3.3). It is stable if all roots of (3.3) have negative real parts and unstable if one root has positive real part. In the following, we will analysis the distribution of characteristic roots of system (3.2).

Firstly, we make the following assumption:

$$(H_3)\quad (\varepsilon+\eta)\left(\frac{2rS^*}{K}+\beta I^*+2\eta-r-\varepsilon\right)+\varepsilon\delta>0.$$

Lemma 1. *Assume that* (H_2) and (H_3) *hold, then the zero equilibrium point* E_0 *of system (3.1) with* $\tau=0$ *is locally asymptotically stable.*

Proof. When $\tau=0$, Eq. (3.3) is equivalent to the following cubic equation:

$$\lambda^3+\left(\frac{2rS^*}{K}+\beta I^*+2\eta+\delta-r\right)\lambda^2$$
$$+\left[(\eta+\delta)\left(\frac{2rS^*}{K}+\beta I^*+\eta-r\right)+\beta^2S^*I^*\right]\lambda$$
$$+\beta I^*(\beta S^*\varepsilon+\beta S^*\delta-\varepsilon\delta)=0.\tag{3.4}$$

Clearly, according to (H_2), we have

$$\frac{2rS^*}{K}+\beta I^*+2\eta+\delta-r>\frac{2rS^*}{K}+\beta I^*+\eta-r$$
$$=\frac{(\eta+\delta)(\eta+\varepsilon)[r(K\beta-\eta-\varepsilon)-K\beta\eta]-\eta(\eta+\varepsilon+\delta)[r(K\beta-2\eta-2\varepsilon-K\beta\eta]}{K\eta\beta^2(\eta+\varepsilon+\delta)}$$
$$>0$$

and

$$(\eta+\delta)\left(\frac{2rS^*}{K}+\beta I^*+\eta-r\right)+\beta^2S^*I^*>0.$$

In addition, under the condition (H_3), it is easy to show that

$$\left(\frac{2rS^*}{K}+\beta I^*+2\eta+\delta-r\right)\left[(\eta+\delta)\left(\frac{2rS^*}{K}+\beta I^*+\eta-r\right)+\beta^2S^*I^*\right]$$
$$-\beta I^*(\beta S^*\varepsilon+\beta S^*\delta-\varepsilon\delta)>0.$$

Furthermore, a simple calculation shows that

$$\beta I^*(\beta S^*\varepsilon+\beta S^*\delta-\varepsilon\delta)=\beta I^*(\eta\varepsilon+\eta\delta+\varepsilon^2)>0.$$

Therefore, by the Routh–Hurwitz criteria, all the roots of Eq. (3.4) have negative real parts. This completes the proof. □

Now we discuss the effect of the delay τ on the stability of E_0. Assume that $i\omega$ is a root of Eq. (3.3). Then ω should satisfy the following equation:

$$-i\omega^3-\left(\frac{2rS^*}{K}+\beta I^*+2\eta-r\right)\omega^2$$
$$+\left[\eta\left(\frac{2rS^*}{K}+\beta I^*+\eta-r\right)+\beta^2S^*I^*\right]i\omega+\beta^2\eta S^*I^*$$
$$+\left[-\omega^2+\left(\frac{2rS^*}{K}+\beta I^*+\eta-r\right)i\omega+\beta^2S^*I^*-\beta I^*\varepsilon\right]$$
$$\times\delta(\cos\ \omega\tau-i\ \sin\ \omega\tau)=0,\tag{3.5}$$

which implies that

$$\begin{cases} \delta\left[(-\omega^2-\beta I^*\varepsilon+\beta^2 S^* I^*)\cos\omega\tau + \left(\frac{2rS^*}{K}+\beta I^*+\eta-r\right)\omega\sin\omega\tau\right] \\ \quad = \left(\frac{2rS^*}{K}+\beta I^*+2\eta-r\right)\omega^2-\beta^2\eta S^* I^*, \\ \delta\left[\left(\frac{2rS^*}{K}+\beta I^*+\eta-r\right)\omega\cos\omega\tau + (\omega^2-\beta^2 S^* I^*+\beta I^*\varepsilon)\sin\omega\tau\right] \\ \quad = \omega^3-\left[\eta\left(\frac{2rS^*}{K}+\beta I^*+\eta-r\right)+\beta^2 S^* I^*\right]\omega, \end{cases} \tag{3.6}$$

taking square on both sides of the equations of (3.6) and summing then up, we obtain

$$\omega^6+(a_1^2+2a_3+\eta^2-\delta^2)\omega^4+(2a_3\eta^2+a_1^2\eta^2 +a_3^2-a_1^2\delta^2-2a_2\delta^2)\omega^2+a_3^2\eta^2-a_2^2\delta^2=0, \tag{3.7}$$

where

$$a_1=\frac{2rS^*}{K}+\beta I^*+\eta-r,\quad a_2=\beta I^*\varepsilon-\beta^2 S^* I^*,\quad a_3=-\beta^2 S^* I^*.$$

Set $z=\omega^2$, Eq. (3.7) is transformed into the following equation:

$$z^3+(a_1^2+2a_3+\eta^2-\delta^2)z^2+(2a_3\eta^2+a_1^2\eta^2+a_3^2-a_1^2\delta^2-2a_2\delta^2)z +a_3^2\eta^2-a_2^2\delta^2=0. \tag{3.8}$$

Denode

$$h(z)=z^3+A_1z^2+A_2z+A_3, \tag{3.9}$$

where

$$A_1=a_1^2+2a_3+\eta^2-\delta^2,\quad A_2=2a_3\eta^2+a_1^2\eta^2+a_3^2-a_1^2\delta^2-2a_2\delta^2,$$
$$A_3=a_3^2\eta^2-a_2^2\delta^2.$$

Furthermore, a simple calculation shows that

$$A_3=\beta\eta I^*(\delta a_2+\eta a_3)(\delta-\eta-\varepsilon).$$

Clearly, the sign of A_3 is consistent with that of $\delta-\eta-\varepsilon$.

Case 1. $\delta-\eta-\varepsilon>0$.

Lemma 2. *If* (H_4) $\delta-\eta-\varepsilon>0$ *holds, then Eq. (3.8) has at least one positive root.*

Proof. According to (H_4), it is easy to show that

$$h(0)=A_3=\beta\eta I^*(\delta a_2+\eta a_3)(\delta-\eta-\varepsilon)<0,\quad \lim_{z\to\infty}h(z)=\infty.$$

Thus, it is obvious that Eq. (3.8) has at least one positive root. This completes the proof. □

Without loss of generality, we assume that it has three positive roots, defined by z_1, z_2, z_3. Then we have

$$\omega_1=\sqrt{z_1},\quad \omega_2=\sqrt{z_2},\quad \omega_3=\sqrt{z_3}.$$

By (3.6), we obtain

$$\cos\omega_k\tau_k=\frac{a_1\omega_k^2(\omega_k^2+a_3-a_1\eta)-(\omega_k^2+a_2)[(a_1+\eta)\omega_k^2+a_3\eta]}{\delta[a_1^2\omega_k^2+(\omega_k^2+a_2)^2]},$$

thus, if we denote

$$\tau_k^j=\frac{1}{\omega_k}\arccos\left(\frac{a_1\omega_k^2(\omega_k^2+a_3-a_1\eta)-(\omega_k^2+a_2)[(a_1+\eta)\omega_k^2+a_3\eta]}{\delta[a_1^2\omega_k^2+(\omega_k^2+a_2)^2]}+2j\pi\right), \tag{3.10}$$

where $k=1,2,3$; $j=0,1,2,\ldots$, then $\pm i\omega_k$ is a pair of purely imaginary roots of (3.3) with τ_k^j. Define

$$\tau_0=\tau_{k_0}^0=\min\{\tau_k^0\},\quad \omega_0=\omega_{k_0}. \tag{3.11}$$

Lemma 3. *[37] Let* $\lambda(\tau)=\alpha(\tau)\pm i\omega(\tau)$ *be the root of (3.3) near* $\tau=\tau_0$ *satisfying* $\alpha(\tau_0)=0$, $\omega(\tau_0)=\omega_0$. *Suppose that* $h'(\omega_0^2)\neq 0$, *where* $h(z)$ *is defined by (3.9). Then* $\pm i\omega_0$ *is a pair of simple purely imaginary roots of Eq. (3.3). Moreover, the following transversality condition holds:*

$$\left.\frac{d(\mathrm{Re}\,\lambda(\tau))}{d\tau}\right|_{\tau=\tau_0,\ \lambda=i\omega_0}\neq 0, \tag{3.12}$$

and the sign of

$$\left.\frac{d(\mathrm{Re}\lambda(\tau))}{d\tau}\right|_{\tau=\tau_0,\lambda=i\omega_0}$$

is consistent with that of $h'(\omega_0^2)$.

Proof. Denote

$$H(\lambda)=\lambda^3+\left(\frac{2rS^*}{K}+\beta I^*+2\eta-r\right)\lambda^2+\left[\eta\left(\frac{2rS^*}{K}+\beta I^*+\eta-r\right)+\beta^2 S^* I^*\right]\lambda +\beta^2\eta S^* I^*,$$

$$G(\lambda)=\left[\lambda^2+\left(\frac{2rS^*}{K}+\beta I^*+\eta-r\right)\lambda+\beta^2 S^* I^*-\beta I^*\varepsilon\right]\delta.$$

Then Eq. (3.3) can be written as

$$H(\lambda)+G(\lambda)e^{-\lambda\tau}=0, \tag{3.13}$$

and Eq. (3.7) is equivalent to:

$$H(i\omega)\overline{H}(i\omega)-G(i\omega)\overline{G}(i\omega)=0. \tag{3.14}$$

Thus, together with (3.8) and (3.9), it is easy to show that

$$h(\omega^2)=H(i\omega)\overline{H}(i\omega)-G(i\omega)\overline{G}(i\omega). \tag{3.15}$$

Differentiating both sides of Eq. (3.15) with respect to ω, we obtain

$$2\omega h'(\omega^2)=i[H'(i\omega)\overline{H}(i\omega)-\overline{H}'(i\omega)H(i\omega)-G'(i\omega)\overline{G}(i\omega)+\overline{G}'(i\omega)G(i\omega)]. \tag{3.16}$$

If $i\omega_0$ is not simple, then ω_0 must satisfy

$$\frac{d}{d\lambda}[H(\lambda)+G(\lambda)e^{-\lambda\tau_0}]|_{\lambda=i\omega_0}=0.$$

That is

$$H'(i\omega_0)+G'(I\omega_0)e^{-i\omega_0\tau_0}-\tau_0G(i\omega_0)e^{-i\omega_0\tau_0}=0.$$

With Eq. (3.13), a simple calculation shows

$$\tau_0=\frac{G'(i\omega_0)}{G(i\omega_0)}-\frac{H'(i\omega_0)}{H(i\omega_0)}.$$

Thus, by (3.14) and (3.16) we obtain

$$\begin{aligned}\mathrm{Im}\,\tau_0&=\mathrm{Im}\left\{\frac{G'(i\omega_0)}{G(i\omega_0)}-\frac{H'(i\omega_0)}{H(i\omega_0)}\right\}\\ &=\mathrm{Im}\left\{\frac{G'(i\omega_0)\overline{G}(i\omega_0)}{G(i\omega_0)\overline{G}(i\omega_0)}-\frac{H'(i\omega_0)\overline{H}(i\omega_0)}{H(i\omega_0)\overline{H}(i\omega_0)}\right\}\\ &=\mathrm{Im}\left\{\frac{G'(i\omega_0)\overline{G}(i\omega_0)-H'(i\omega_0)\overline{H}(i\omega_0)}{H(i\omega_0)\overline{H}(i\omega_0)}\right\}\\ &=\frac{i[G'(i\omega_0)\overline{G}(i\omega_0)-H'(i\omega_0)\overline{H}(i\omega_0)-\overline{G}'(i\omega_0)G(i\omega_0)+\overline{H}'(i\omega_0)H(i\omega_0)]}{2H(i\omega_0)\overline{H}(i\omega_0)}\\ &=\frac{\omega_0h'(\omega_0^2)}{|H(i\omega_0)|^2}.\end{aligned}$$

Since τ_0 is real, i.e. $\mathrm{Im}\,\tau_0=0$, we have

$$h'(\omega_0^2)=0.$$

We get a contradiction to the condition $h'(\omega_0^2)\neq 0$. This proves the first conclusion. Differentiating both sides of Eq. (3.13) with respect to τ, we obtain

$$[H'(\lambda)+G'(\lambda)e^{-\lambda\tau}-\tau G(\lambda)e^{-\lambda\tau}]\frac{d\lambda}{d\tau}-\lambda G(\lambda)e^{-\lambda\tau}=0,$$

which implies

$$\begin{aligned}
&\mathrm{Re}\left[\frac{d(\lambda(\tau))}{d\tau}\right]^{-1}\Big|_{\tau=\tau_0,\ \lambda=i\omega_0} = \mathrm{Re}\left[\frac{H'(\lambda)e^{\lambda\tau}+G'(\lambda)}{\lambda G(\lambda)}-\frac{\tau}{\lambda}\Big|_{\tau=\tau_0,\ \lambda=i\omega_0}\right]\\
&= \mathrm{Re}\left[\frac{[H'(\lambda)e^{\lambda\tau}+G'(\lambda)]\overline{\lambda}\,\overline{G}(\lambda)}{|\lambda G(\lambda)|^2}-\frac{\tau}{\lambda}\Big|_{\tau=\tau_0,\ \lambda=i\omega_0}\right]\\
&= \mathrm{Re}\left[\frac{i\omega_0[H'(i\omega_0)\overline{F}(i\omega_0)-G'(i\omega_0)\overline{G}(i\omega_0)]}{|i\omega_0 G(i\omega_0)|^2}-\frac{\tau}{i\omega_0}\right]\\
&= \frac{i\omega_0[H'(i\omega_0)\overline{H}(i\omega_0-\overline{H}'(i\omega_0)H(i\omega_0)-G'(i\omega_0)\overline{G}(i\omega_0)+\overline{G}'(i\omega_0)G(i\omega_0)]}{2|i\omega_0 G(i\omega_0)|^2}\\
&= \frac{\omega_0^2 h'(\omega_0^2)}{|i\omega_0 G(i\omega_0)|^2}\neq 0.
\end{aligned}$$

Clearly, the sign of

$$\frac{d(\mathrm{Re}\lambda(\tau))}{d\tau}\Big|_{\tau=\tau_0,\lambda=i\omega_0}$$

is determined by that of $h'(\omega_0^2)$. This completes the proof. □

Applying Lemmas 1–3, it is easy to obtain the following conclusion.

Theorem 1. *Let τ_k^j and τ_0 be defined by (3.10) and (3.11), respectively. If (H_2)–(H_4) hold. Assume furthermore that the conditions of Lemma 3 are satisfied. Then for system (3.1), the following statements are true:*

(i) *When $\tau\in[0,\tau_0)$, the zero equilibrium point E_0 of system (3.1) is locally asymptotically stable.*
(ii) *The Hopf bifurcation occurs when $\tau=\tau_k^j$. That is, system (3.1) has a branch of periodic solutions bifurcating from the zero equilibrium point E_0 near $\tau=\tau_k^j$.*

Case 2. $\delta-\eta-\varepsilon\le 0$.

In this case, the discussion about the roots of Eq. (3.8) is similar to that of Wei [30], we have the following lemma.

Lemma 4. *If* (H_5) $\delta-\eta-\varepsilon\le 0$, $\Delta=A_1^2-3A_2>0$, $z^*=(-A_1+\sqrt{\Delta})/3>0$, $h(z^*)\le 0$ *holds, then Eq. (3.8) has positive roots.*

Furthermore, according to Descartes' rule of signs [31], it is easy to show that Eq. (3.8) has two positive roots. Without loss of generality, we assume that Z_1 and Z_2 are the two positive roots, and $Z_1>Z_2$. Then we have

$$\omega_1=\sqrt{Z_1}>\omega_2=\sqrt{Z_2}.$$

By (3.6), we obtain

$$\cos\ \omega_l\tau_l=\frac{a_1\omega_l^2(\omega_l^2+a_3-a_1\eta)-(\omega_l^2+a_2)[(a_1+\eta)\omega_l^2+a_3\eta]}{\delta[a_1^2\omega_l^2+(\omega_l^2+a_2)^2]}\quad(l=1,2),$$

thus

$$\tau_{n,1}=\frac{1}{\omega_1}\arccos\left(\frac{a_1\omega_1^2(\omega_1^2+a_3-a_1\eta)-(\omega_1^2+a_2)[(a_1+\eta)\omega_1^2+a_3\eta]}{\delta[a_1^2\omega_1^2+(\omega_1^2+a_2)^2]}+2n\pi\right),\tag{3.17}$$

$$\tau_{n,2}=\frac{1}{\omega_2}\arccos\left(\frac{a_1\omega_1^2(\omega_2^2+a_3-a_1\eta)-(\omega_2^2+a_2)[(a_1+\eta)\omega_2^2+a_3\eta]}{\delta[a_1^2\omega_2^2+(\omega_2^2+a_2)^2]}+2n\pi\right),\tag{3.18}$$

where $n=0,1,2,\ldots$, then $\pm i\omega_l$ is a pair of purely imaginary roots of (3.3) with $\tau=\tau_{n,l}$. Furthermore, similar to Lemma 3 we can easily prove that $\pm i\omega_l$ is a pair of simple purely imaginary roots of Eq. (3.3).

Theorem 2. *If (H_2)–(H_3) and (H_5) hold. Assume furthermore that $h'(Z_1)>0$ and $h'(Z_2)<0$. Then for system (3.1), there is a positive integer m, such that the zero equilibrium point E_0 switches m times from stability to instability to stability; that is, E_0 is locally asymptotically stable when*

$$\tau\in[0,\tau_{0,1})\cup(\tau_{0,2},\tau_{1,1})\cup\cdots\cup(\tau_{m-1,2},\tau_{m,1}),$$

and unstable when

$$\tau\in(\tau_{0,1},\tau_{0,2})\cup(\tau_{1,1},\tau_{1,2})\cup\cdots\cup(\tau_{m-1,1},\tau_{m-1,2})\quad\text{and}\quad\tau>\tau_{m,1}.$$

System (3.1) undergoes a Hopf bifurcation at E_0 when $\tau=\tau_{n,l}$ $(l=1,2;\ n=0,1,2\ldots)$, where $\tau=\tau_{n,l}$ is defined by (3.17) and (3.18).

Proof. Similar to Lemma 3, it is easy to show that $\pm i\omega_l$ is a pair of simple purely imaginary roots of Eq. (3.3). Moreover, the following transversality conditions hold:

$$\frac{d(\mathrm{Re}\ \lambda(\tau))}{d\tau}\Big|_{\tau=\tau_{n,1},\ \lambda=i\omega_1}>0\quad\text{and}\quad\frac{d(\mathrm{Re}\ \lambda(\tau))}{d\tau}\Big|_{\tau=\tau_{n,2},\ \lambda=i\omega_2}<0.$$

Thus, for system (3.1), at each value $\tau=\tau_{n,1}$, a pair of roots crosses the imaginary axis at $i\omega_1$ into the right half-plane, and at each $\tau=\tau_{n,2}$, a pair of roots crosses at $i\omega_2$ back into the left-plane. According to the discussion above, we can see that the phenomenon of stability switches occurs with τ increasing. Next we will prove that the phenomenon of stability switches can be found in a finite number.

In fact, we note immediately that since

$$\tau_{n+1,1}-\tau_{n,1}=\frac{2\pi}{\omega_1},\quad\tau_{n+1,2}-\tau_{n,2}=\frac{2\pi}{\omega_2}$$

and $\omega_1>\omega_2$, this alternation cannot persist for the whole of the sequences. Eventually, therefore, there is an integer m such that

$$\tau_{m-1,1}<\tau_{m-1,2}<\tau_{m,1}<\tau_{m+1,1}<\tau_{m,2}.$$

Hence for $\tau>\tau_{m,1}$, the multiplicity of roots in the right half-plane is at least two and the system is unstable. This proves Theorem 2. □

4. Properties of bifurcating periodic oscillations

In the previous section, we have shown that system (3.1) admits a series of periodic solutions bifurcating from the zero equilibrium point E_0 at the critical value τ_k^j $(j\in N_0)$. As we all know, the periodic oscillation in the wireless sensor networks may destroy, block regular communications, or even damage the integrity of regular data packets. Thus, understanding the properties of the periodic oscillation, such as stability, direction and monotonicity of the periodicity, is necessary. In this section, we derive explicit formulae to determine the properties of the Hopf bifurcation at critical value τ_k^j $(j\in N_0)$ by using the normal form theory and center manifold reduction for PFDEs developed by [32–34].

In this section, let $U(t)=(u_1(t),u_2(t),u_3(t))^T=(S(t),I(t),R(t))^T$. For fixed $j\in N_0$, denote τ_k^j by τ^* and introduce the new parameter $\mu=\tau-\tau^*$. Normalizing the delay τ by the time-scaling $t\to t/\tau$. Then (3.1) can be written as a functional differential equation (FDE) in $\mathcal{C}=\mathcal{C}([-1,0],\mathbb{R}^3)$

$$\frac{dU(t)}{dt}=L(\tau^*)(U_t)+F(U_t,\mu),\tag{4.1}$$

where $L(\mu)(\varphi):\mathcal{C}\to\mathbb{R}^3$ and $F(\cdot,\mu):\mathcal{C}\times\mathbb{R}\to\mathbb{R}^3$ are given by

$$L(\mu)(\varphi)=\mu\begin{pmatrix}(-\beta I^*-\eta)\varphi_1(0)-\beta S^*\varphi_2(0)+\delta\varphi_3(-1)\\ \beta I^*\varphi_1(0)+(\beta S^*-\varepsilon-k_1)\varphi_2(0)\\ \varepsilon\varphi_2(0)-\eta\varphi_3(0)-\delta\varphi_3(-1)\end{pmatrix},\tag{4.2}$$

$$F(\varphi,\mu)=L(\mu)\varphi+f(\varphi,\mu)\tag{4.3}$$

and

$$f(\varphi,\mu)=(\tau^*+\mu)\begin{pmatrix}-\beta\varphi_1(0)\varphi_2(0)-\frac{r}{K}\varphi_1^2(0)\\ \beta\varphi_1(0)\varphi_2(0)\\ 0\end{pmatrix}, \tag{4.4}$$

for $\varphi=(\varphi_1,\varphi_2,\varphi_3)^T\in\mathcal{C}$.

Then linearized system of (4.1) at E_0 is

$$\frac{dU(t)}{dt}=L(\tau^*)(U_t). \tag{4.5}$$

Obviously, $L(\tau^*)$ is a continuous linear function mapping $\mathcal{C}([-1,0],\mathbb{R}^3)$ into $\mathbb{R}^3$. By the Riesz representation theorem, there exists a 3×3 matrix function $\eta(\theta,\tau)$ $(-1\le\theta\le0)$, whose elements are of bounded variation such that

$$L(\tau^*)(\varphi)=\int_{-1}^{0}[d\eta(\theta,\tau^*)]\varphi(\theta)\quad\text{for }\varphi\in\mathcal{C}. \tag{4.6}$$

In fact, we can choose

$$\eta(\theta,\tau^*)=\tau^*\begin{pmatrix}r-\frac{2rS^*}{K}-\beta I^*-\eta & -\beta S^* & 0\\ \beta I^* & \beta S^*-\varepsilon-\eta & 0\\ 0 & \varepsilon & -\eta\end{pmatrix}\nu(\theta)-\tau^*\begin{pmatrix}0&0&\delta\\0&0&0\\0&0&-\delta\end{pmatrix}\nu(\theta+1), \tag{4.7}$$

where ν is the Dirac delta function.

Let $A(\tau^*)$ denote the infinitesimal generator of the semigroup induced by the solutions of (4.5) and A^* be the formal adjoint of $A(\tau^*)$ under the bilinear pairing

$$\begin{aligned}(\psi,\phi)&=(\psi(0),\phi(0))-\int_{-1}^{0}\int_{\zeta=0}^{\theta}\psi(\zeta-\theta)\,d\eta(\theta)\phi(\zeta)\,d\zeta\\&=(\psi(0),\phi(0))+\tau^*\int_{-1}^{0}\psi(\theta+1)\begin{pmatrix}0&0&\delta\\0&0&0\\0&0&-\delta\end{pmatrix}\phi(\theta)\,d\theta,\end{aligned} \tag{4.8}$$

for $\phi,\psi\in\mathcal{C}$. Then $A(\tau^*)$ and A^* are a pair of adjoint operators [32]. From the discussion in Section 3, we know that $A(\tau^*)$ has a pair of simple purely imaginary eigenvalues $\pm i\omega_0\tau^*$ and they are also eigenvalues of A^* since $A(\tau^*)$ and A^* are a pair of adjoint operators. Let P and P^* be the center spaces, that is, the generalized eigenspaces of $A(\tau^*)$ and A^* associated with Λ_0, respectively. Then P^* is the adjoint space of P and $dim\,P=dim\,P^*=2$. Direct computations give the following results.

Lemma 5. *Let*

$$\begin{cases}\xi=\dfrac{\beta I^*}{i\omega_0}, & \varsigma=\dfrac{\beta\varepsilon I^*}{i\omega_0(\eta+\delta e^{-i\omega_0\tau^*}+i\omega_0)},\\ \xi^*=\dfrac{\delta\varepsilon-\beta S^*(i\omega_0+\delta+\eta)}{i\omega_0(i\omega_0+\delta+\eta)}, & \varsigma^*=\dfrac{\delta}{i\omega_0+\delta+\eta}.\end{cases} \tag{4.9}$$

Then

$$p_1(\theta)=e^{i\omega_0\tau^*\theta}(1,\xi,\varsigma)^T,\quad p_2(\theta)=\overline{p_1(\theta)},\quad -1\le\theta\le0 \tag{4.10}$$

is a basis of P associated with Λ_0 and

$$q_1(s)=(1,\xi^*,\varsigma^*)e^{-i\omega_0\tau^*s},\quad q_2(s)=\overline{q_1(s)},\quad 0\le s\le1 \tag{4.11}$$

is a basis of Q associated with Λ_0.

Let $\Phi=(\Phi_1,\Phi_2)$ and $\Psi^*=(\Psi_1^*,\Psi_2^*)^T$ with

$$\Phi_1(\theta)=\frac{p_1(\theta)+p_2(\theta)}{2}=\begin{pmatrix}\mathrm{Re}\{e^{i\omega_0\tau^*\theta}\}\\ \mathrm{Re}\{\xi e^{i\omega_0\tau^*\theta}\}\\ \mathrm{Re}\{\varsigma e^{i\omega_0\tau^*\theta}\}\end{pmatrix}$$

$$=\begin{pmatrix}\cos\ \omega_0\tau^*\theta\\ \dfrac{\beta I^*}{\omega_0}\ \sin\ \omega_0\tau^*\theta\\ \dfrac{\beta I^*\varepsilon\ \cos\ \omega_0\tau^*\theta(\delta\ \sin\ \omega_0\tau^*-\omega_0)+\beta I^*\varepsilon\ \sin\ \omega_0\tau^*\theta(\eta+\delta\ \cos\ \omega_0\tau^*)}{\omega_0[(\eta+\delta\ \cos\ \omega_0\tau^*)^2+(\delta\ \sin\ \omega_0\tau^*-\omega_0)^2]}\end{pmatrix},$$

$$\Phi_2(\theta)=\frac{p_1(\theta)-p_2(\theta)}{2i}=\begin{pmatrix}\mathrm{Im}\{e^{i\omega_0\tau^*\theta}\}\\ \mathrm{Im}\{\xi e^{i\omega_0\tau^*\theta}\}\\ \mathrm{Im}\{\varsigma e^{i\omega_0\tau^*\theta}\}\end{pmatrix}$$

$$=\begin{pmatrix}\sin\ \omega_0\tau^*\theta\\ -\dfrac{\beta I^*}{\omega_0}\ \cos\ \omega_0\tau^*\theta\\ \dfrac{\beta I^*\varepsilon\ \sin\ \omega_0\tau^*\theta(\delta\ \sin\ \omega_0\tau^*-\omega_0)-\beta I^*\varepsilon\ \cos\ \omega_0\tau^*\theta(\eta+\delta\ \cos\ \omega_0\tau^*)}{\omega_0[(\eta+\delta\ \cos\ \omega_0\tau^*)^2+(\delta\ \sin\ \omega_0\tau^*-\omega_0)^2]}\end{pmatrix}$$

and

$$\Psi_1^*(s)=\frac{q_1(s)+q_2(s)}{2}=\begin{pmatrix}\mathrm{Re}\{e^{-i\omega_0\tau^*s}\}\\ \mathrm{Re}\{\xi^*e^{-i\omega_0\tau^*s}\}\\ \mathrm{Re}\{\varsigma^*e^{-i\omega_0\tau^*s}\}\end{pmatrix}^T$$

$$=\begin{pmatrix}\cos\ \omega_0\tau^*s\\ \dfrac{-\delta\varepsilon\omega_0\ \cos\ \omega_0\tau^*s+\sin\ \omega_0\tau^*s[\beta S^*(\eta+\delta)^2+\beta S^*\omega_0^2-\delta\varepsilon(\eta+\delta)]}{\omega_0[(\eta+\delta)^2+\omega_0^2]}\\ \dfrac{\delta(\eta+\delta)\ \cos\ \omega_0\tau^*s-\delta\omega_0\ \sin\ \omega_0\tau^*s}{(\eta+\delta)^2+\omega_0^2}\end{pmatrix}^T,$$

$$\Psi_2^*(s)=\frac{q_1(s)-q_2(s)}{2i}=\begin{pmatrix}\mathrm{Im}\{e^{-i\omega_0\tau^*s}\}\\ \mathrm{Im}\{\xi^*e^{-i\omega_0\tau^*s}\}\\ \mathrm{Im}\{\varsigma^*e^{-i\omega_0\tau^*s}\}\end{pmatrix}^T$$

$$=\begin{pmatrix}-\sin\ \omega_0\tau^*s\\ \dfrac{\delta\varepsilon\omega_0\ \sin\ \omega_0\tau^*s+\cos\ \omega_0\tau^*s[\beta S^*(\eta+\delta)^2+\beta S^*\omega_0^2-\delta\varepsilon(\eta+\delta)]}{\omega_0[(\eta+\delta)^2+\omega_0^2]}\\ \dfrac{-\delta(\eta+\delta)\sin\ \omega_0\tau^*s-\delta\omega_0\ \cos\ \omega_0\tau^*s}{(\eta+\delta)^2+\omega_0^2}\end{pmatrix}^T,$$

for $s\in[0,1]$. From (4.8), we can obtain (Ψ_1^*,Φ_1) and (Ψ_1^*,Φ_2). Noting that

$$(q_1,p_1)=(\Psi_1^*,\Phi_1)-(\Psi_2^*,\Phi_2)+i[(\Psi_1^*,\Phi_2)+(\Psi_2^*,\Phi_1)]$$

and

$$(q_1,p_1)=1+\xi\xi^*+\varsigma\varsigma^*+\tau^*\delta\varsigma e^{-i\omega_0\tau^*}(1-\varsigma^*):=D^*.$$

Therefore, we have

$$(\Psi_1^*,\Phi_1)-(\Psi_2^*,\Phi_2)=\mathrm{Re}\{D^*\},$$
$$(\Psi_1^*,\Phi_2)+(\Psi_2^*,\Phi_1)=\mathrm{Im}\{D^*\}.$$

Now, we define $(\Psi^*,\Phi)=(\Psi_j^*,\Phi_k)$ $(j,k=1,2)$ and construct a new basis Ψ for Q by $\Psi=(\Psi_1,\Psi_2)^T=(\Psi^*,\Phi)^{-1}\Psi^*$.

Obviously, (Ψ,Φ) is a second order identity matrix. In addition, define $f_0=(\beta_0^1,\beta_0^2,\beta_0^3)^T$, where

$$\beta_0^1=\begin{pmatrix}1\\0\\0\end{pmatrix},\quad \beta_0^2=\begin{pmatrix}0\\1\\0\end{pmatrix},\quad \beta_0^3=\begin{pmatrix}0\\0\\1\end{pmatrix}.$$

Let $c\cdot f_0$ be defined by

$$c\cdot f_0=c_1\beta_0^1+c_2\beta_0^2+c_3\beta_0^3,$$

for $c=(c_1,c_2,c_3)^T$, $c_j\in\mathbb{R}$ $(j=1,2,3)$.

Then the center space of linear equation (4.5) is given by $P_{CN}\mathcal{C}$, where

$$P_{CN}\varphi = \Phi(\Psi, \langle \varphi, f_0 \rangle) \cdot f_0, \quad \varphi \in \mathcal{C} \tag{4.12}$$

and

$$\mathcal{C} = P_{CN}\mathcal{C} \oplus P_S\mathcal{C},$$

here $P_S\mathcal{C}$ denotes the complementary subspace of $P_{CN}\mathcal{C}$.

Let

$$W(z,\bar{z}) = W_{20}\frac{z^2}{2} + W_{11}z\bar{z} + W_{02}\frac{\bar{z}^2}{2} + \cdots \tag{4.22}$$

and

$$g(z,\bar{z}) = g_{20}\frac{z^2}{2} + g_{11}z\bar{z} + g_{02}\frac{\bar{z}^2}{2} + \cdots. \tag{4.23}$$

From (4.19), we have

$$\begin{aligned}\langle F(U_t^*,0), f_0\rangle = {} & \frac{\tau^*}{4}\begin{pmatrix} -(\beta\xi + \frac{r}{K})z^2 - [\beta(\xi+\bar{\xi}) + \frac{2r}{K}]z\bar{z} - (\beta\bar{\xi} + \frac{r}{K})\bar{z}^2 \\ \beta\xi z^2 + (\beta\xi + \beta\bar{\xi})z\bar{z} + \beta\bar{\xi}\bar{z}^2 \\ 0 \end{pmatrix} \\ & + \frac{\tau^*}{4}\begin{pmatrix} \langle -\beta(2W_{11}^{(2)}(0) + W_{20}^{(2)}(0) + \bar{\xi}W_{20}^{(1)}(0) + 2\xi W_{11}^{(1)}(0)) - \frac{2r}{K}(2W_{11}^{(1)}(0) + W_{20}^{(1)}(0)), 1\rangle \\ \langle \beta(2W_{11}^{(2)}(0) + W_{20}^{(2)}(0) + \bar{\xi}W_{20}^{(1)}(0) + 2\xi W_{11}^{(1)}(0)), 1\rangle \\ 0 \end{pmatrix} z^2\bar{z} + \cdots,\end{aligned}$$

Let A_{τ^*} be defined by

$$A_{\tau^*}\varphi(\theta) = \dot{\varphi}(\theta) + X_0(\theta)[L(\tau^*)(\varphi(\theta)) - \dot{\varphi}(0)], \quad \varphi \in \mathcal{C}, \tag{4.13}$$

where X_0 is given by

$$X_0(\theta) = \begin{cases} 0, & -1 \le \theta < 0, \\ I, & \theta = 0. \end{cases} \tag{4.14}$$

Then A_{τ^*} is the infinitesimal generator induced by the solution of (4.5) and (4.1) can be rewritten as the following operator differential equation:

$$\dot{U}_t = A_{\tau^*}U_t + X_0F(U_t, \mu). \tag{4.15}$$

Using the decomposition $\mathcal{C} = P_{CN}\mathcal{C} \oplus P_S\mathcal{C}$ and (4.12), the solution of (4.1) can be rewritten as

$$U_t = \Phi\begin{pmatrix} x_1(t) \\ x_2(t) \end{pmatrix} \cdot f_0 + h(x_1, x_2, \mu), \tag{4.16}$$

where

$$\begin{pmatrix} x_1(t) \\ x_2(t) \end{pmatrix} = (\Psi, \langle U_t, f_0 \rangle), \tag{4.17}$$

and $h(x_1, x_2, \mu) \in P_sC$ with $h(0,0,0) = Dh(0,0,0) = 0$. In particular, the solution of (4.1) on the center manifold is given by

$$U_t^* = \Phi\begin{pmatrix} x_1(t) \\ x_2(t) \end{pmatrix} \cdot f_0 + h(x_1, x_2, 0). \tag{4.18}$$

Setting $z = x_1 - ix_2$ and noticing that $p_1 = \Phi_1 + i\Phi_2$, then (4.18) can be rewritten as

$$U_t^* = \frac{1}{2}\Phi\begin{pmatrix} z+\bar{z} \\ i(z-\bar{z}) \end{pmatrix} \cdot f_0 + w(z,\bar{z}) = \frac{1}{2}(p_1 z + \overline{p_1 z}) \cdot f_0 + W(z,\bar{z}), \tag{4.19}$$

where $W(z,\bar{z}) = h((z+\bar{z})/2, -(z-\bar{z})/2i, 0)$. Moreover, by [32], z satisfies

$$\dot{z} = i\omega_0\tau^* z + g(z,\bar{z}), \tag{4.20}$$

where

$$g(z,\bar{z}) = (\Psi_1(0) - i\Psi_2(0))\langle F(U_t^*, 0), f_0\rangle. \tag{4.21}$$

where

$$\langle W_{ij}^n(\theta), 1\rangle = \frac{1}{\pi}\int_0^\pi W_{ij}^n(\theta)(x)\, dx, \quad i+j = 2, \ n \in \mathbb{N}.$$

Let $(\psi_1, \psi_2) = \Psi_1(0) - i\Psi_2(0)$. Then by (4.20)–(4.22), we can obtain the following quantities:

$$g_{20} = \frac{\tau^*}{2}\Big[-\Big(\beta\xi + \frac{r}{K}\Big)\psi_1 + \beta\xi\psi_2\Big],$$

$$g_{11} = \frac{\tau^*}{4}\Big[-\Big(\beta\bar{\xi} + \beta\xi + \frac{2r}{K}\Big)\psi_1 + (\beta\bar{\xi} + \beta\xi)\psi_2\Big],$$

$$g_{02} = \frac{\tau^*}{2}\Big[-\Big(\beta\bar{\xi} + \frac{r}{K}\Big)\psi_1 + \beta\bar{\xi}\psi_2\Big],$$

$$\begin{aligned} g_{21} = \frac{\tau^*}{2}\Big[\Big\langle & -\beta\Big(2W_{11}^{(2)}(0) + W_{20}^{(2)}(0) + \bar{\xi}W_{20}^{(1)}(0) + 2\xi W_{11}^{(1)}(0)\Big) \\ & -\frac{2r}{K}\Big(2W_{11}^{(1)}(0) + W_{20}^{(1)}(0)\Big), 1\Big\rangle\psi_1 \\ & + \langle\beta(2W_{11}^{(2)}(0) + W_{20}^{(2)}(0) + \bar{\xi}W_{20}^{(1)}(0) + 2\xi W_{11}^{(1)}(0)), 1\rangle\psi_2\Big]. \end{aligned}$$

Since $W_{20}(\theta), W_{11}(\theta)$ for $\theta \in [-1, 0]$ appear in g_{21}, we still need to compute them. It easily follows from (4.21) that

$$\dot{W}(z,\bar{z}) = W_{20}z\dot{z} + W_{11}(\dot{z}\bar{z} + z\dot{\bar{z}}) + W_{02}\bar{z}\dot{\bar{z}} + \cdots \tag{4.24}$$

and

$$A_{\tau^*}W = A_{\tau^*}W_{20}\frac{z^2}{2} + A_{\tau^*}W_{11}z\bar{z} + A_{\tau^*}W_{02}\frac{\bar{z}^2}{2} + \cdots. \tag{4.25}$$

In addition, by [32], $W(z(t), \bar{z}(t))$ satisfies

$$\dot{W} = A_{\tau^*}W + H(z,\bar{z}), \tag{4.26}$$

where

$$\begin{aligned} H(z,\bar{z}) &= H_{20}\frac{z^2}{2} + H_{11}z\bar{z} + H_{02}\frac{\bar{z}^2}{2} + \cdots \\ &= X_0F(U_t^*, 0) - \Phi(\Psi, \langle X_0F(U_t^*, 0), f_0\rangle) \cdot f_0, \end{aligned}$$

with $H_{ij} \in P_S\mathcal{C}$, $i+j = 2$.

Thus, from (4.18) and (4.23)–(4.25), we can obtain that

$$\begin{cases} (2i\omega_0\tau^* - A_{\tau^*})W_{20} = H_{20}, \\ -A_{\tau^*}W_{11} = H_{11}. \end{cases} \tag{4.27}$$

Noticing that A_{τ^*} has only two eigenvalues $\pm i\omega_0\tau^*$ with zero real parts, therefore, (4.25) has unique solution $W_{ij}(i+j=2)$ in $P_S\mathcal{C}$ given by

$$\begin{cases} W_{20} = (2i\omega_0\tau^* - A_{\tau^*})^{-1} H_{20}, \\ W_{11} = -A_{\tau^*}^{-1} H_{11}. \end{cases} \tag{4.28}$$

From (4.26), we know that for $-1 \le \theta < 0$,

$$\begin{aligned} H(z,\bar{z}) &= -\Phi(\theta)\Psi(0) < F(U_t^*,0), f_0 > \cdot f_0 \\ &= -\left(\frac{p_1(\theta)+p_2(\theta)}{2}, \frac{p_1(\theta)-p_2(\theta)}{2i}\right)(\Psi_1(0),\Psi_2(0))^T \times \langle F(U_t^*,0), f_0\rangle \cdot f_0 \\ &= -\frac{1}{2}[p_1(\theta)(\Psi_1(0) - i\Psi_2(0)) + p_2(\theta)(\Psi_1(0) + i\Psi_2(0))] \times \langle F(U_t^*,0), f_0\rangle \cdot f_0 \\ &= -\frac{1}{4}[g_{20}p_1(\theta) + \bar{g}_{02}p_2(\theta)]z^2 \cdot f_0 - \frac{1}{2}[g_{11}p_1(\theta) + \bar{g}_{11}p_2(\theta)]z\bar{z} \cdot f_0 + \cdots \end{aligned}$$

Therefore, for $-1 \le \theta < 0$,

$$H_{20}(\theta) = -\tfrac{1}{2}[g_{20}p_1(\theta) + \bar{g}_{02}p_2(\theta)] \cdot f_0, \tag{4.29}$$

$$H_{11}(\theta) = -\tfrac{1}{2}[g_{11}p_1(\theta) + \bar{g}_{11}p_2(\theta)] \cdot f_0 \tag{4.30}$$

and

$$H(z,\bar{z})(0) = F(U_t^*,0) - \Phi(\Psi, \langle F(U_t^*,0), f_0\rangle) \cdot f_0,$$

$$H_{20}(0) = \frac{\tau^*}{2}\begin{pmatrix} -\beta\xi - \frac{r}{K} \\ \beta\xi \\ 0 \end{pmatrix} - \frac{1}{2}[g_{20}p_1(0) + \bar{g}_{02}p_2(0)] \cdot f_0, \tag{4.31}$$

$$H_{11}(0) = \frac{\tau^*}{4}\begin{pmatrix} -\beta\bar{\xi} - \beta\xi - \frac{2r}{K} \\ \beta\bar{\xi} + \beta\xi \\ 0 \end{pmatrix} - \frac{1}{2}[g_{11}p_1(0) + \bar{g}_{11}p_2(0)] \cdot f_0. \tag{4.32}$$

By the definition of A_{τ^*}, we get from (4.27) that

$$\dot{W}_{20}(\theta) = 2i\omega_0\tau^* W_{20}(\theta) + \tfrac{1}{2}[g_{20}p_1(\theta) + \bar{g}_{02}p_2(\theta)] \cdot f_0, \quad -1 \le \theta < 0.$$

Noting that $p_1(\theta) = p_1(0)e^{i\omega_0\tau^*}$, $-1 \le \theta \le 0$. Hence

$$W_{20}(\theta) = \frac{i}{2}\left[\frac{g_{20}}{\omega_0\tau^*}p_1(\theta) + \frac{\bar{g}_{02}}{3\omega_0\tau^*}p_2(\theta)\right] \cdot f_0 + Ee^{2i\omega_0\tau^*\theta} \tag{4.33}$$

and

$$E = W_{20}(0) - \frac{i}{2}\left[\frac{g_{20}}{\omega_0\tau^*}p_1(0) + \frac{\bar{g}_{02}}{3\omega_0\tau^*}p_2(0)\right] \cdot f_0. \tag{4.34}$$

Using the definition of A_{τ^*}, and combining (4.27) and (4.33), we get

$$\begin{aligned} &2i\omega_0\tau^*\left[\frac{ig_{20}}{2\omega_0\tau^*}p_1(0) \cdot f_0 + \frac{i\bar{g}_{02}}{6\omega_0\tau^*}p_2(0) \cdot f_0 + E\right] \\ &\quad - L(\tau^*)\left[\frac{ig_{20}}{2\omega_0\tau^*}p_1(\theta) \cdot f_0 + \frac{i\bar{g}_{02}}{6\omega_0\tau^*}p_2(\theta) \cdot f_0 + Ee^{2i\omega_0\tau^*\theta}\right] \\ &= \frac{\tau^*}{2}\begin{pmatrix} -\beta\xi - \frac{r}{K} \\ \beta\xi \\ 0 \end{pmatrix} - \frac{1}{2}[g_{20}p_1(0) + \bar{g}_{02}p_2(0)] \cdot f_0. \end{aligned}$$

Notice that

$$\begin{cases} L(\tau^*)[p_1(\theta) \cdot f_0] = i\omega_0\tau^* p_1(0) \cdot f_0, \\ L(\tau^*)[p_2(\theta) \cdot f_0] = -i\omega_0\tau^* p_2(0) \cdot f_0. \end{cases}$$

Then

$$2i\omega_0\tau^* E - L(\tau^*)(Ee^{2i\omega_0\tau^*\theta}) = \frac{\tau^*}{2}\begin{pmatrix} -\beta\xi - \frac{r}{K} \\ \beta\xi \\ 0 \end{pmatrix}.$$

From the above expression, we can see easily that

$$E = \frac{1}{2}\begin{pmatrix} 2i\omega_0 + \frac{2rS^*}{K} + \eta + \beta I^* - r & \beta S^* & -\delta \\ -\beta I^* & 2i\omega_0 + \varepsilon + \eta - \beta S^* & 0 \\ 0 & -\varepsilon & 2i\omega_0 + \eta + \delta \end{pmatrix}^{-1} \times \begin{pmatrix} -\beta\xi - \frac{r}{K} \\ \beta\xi \\ 0 \end{pmatrix}.$$

In a similar way, we have

$$\dot{W}_{11}(\theta) = \tfrac{1}{2}[g_{11}p_1(\theta) + \bar{g}_{11}p_2(\theta)] \cdot f_0, \quad -1 \le \theta < 0$$

and

$$W_{11}(\theta) = \frac{i}{2\omega_0\tau^*}[-g_{11}p_1(\theta) + \bar{g}_{11}p_2(\theta)] \cdot f_0 + F.$$

Similar to the above, we can obtain that

$$F = \frac{1}{4}\begin{pmatrix} \frac{2rS^*}{K} + \eta + \beta I^* - r & \beta S^* & -\delta \\ -\beta I^* & \eta + \varepsilon - \beta S^* & 0 \\ 0 & -\varepsilon & \eta + \delta \end{pmatrix}^{-1} \times \begin{pmatrix} m - \beta\bar{\xi} - \beta\xi - \frac{2r}{K} \\ \beta\bar{\xi} + \beta\xi \\ 0 \end{pmatrix}.$$

So far, $W_{20}(\theta)$ and $W_{11}(\theta)$ have been expressed by the parameters of system (3.1), Therefore, g_{21} can be expressed explicitly.

Theorem 3. *System (3.1) have the following Poincaré normal form:*

$$\dot{\varrho} = i\omega_0\tau^*\varrho + c_1(0)\varrho|\varrho|^2 + o(|\varrho|^5),$$

where

$$c_1(0) = \frac{i}{2\omega_0\tau^*}\left(g_{20}g_{11} - 2|g_{11}|^2 - \frac{|g_{02}|^2}{3}\right) + \frac{g_{21}}{2},$$

so we can compute the following result:

$$\sigma_2 = -\frac{\mathrm{Re}(c_1(0))}{\mathrm{Re}(\lambda'(\tau^*))},$$

$$\beta_2 = 2\,\mathrm{Re}(c_1(0)),$$

$$T_2 = -\frac{\mathrm{Im}(c_1(0)) + \sigma_2\,\mathrm{Im}(\lambda'(\tau^*))}{\omega_0\tau^*},$$

which determine the properties of bifurcating periodic solutions at the critical values τ^*, i.e., σ_2 determines the directions of the Hopf bifurcation: if $\sigma_2 > 0$ ($\sigma_2 < 0$), then the Hopf bifurcation is supercritical (subcritical) and the bifurcating periodic solutions exist for $\tau > \tau^*$; β_2 determines the stability of the bifurcating periodic solutions: the bifurcating periodic solutions on the center manifold are stable (unstable), if $\beta_2 < 0$ ($\beta_2 > 0$); and T_2 determines the period of the bifurcating periodic solutions: the periodic increase(decrease), if $T_2 > 0$ ($T_2 < 0$).

5. Optimal control strategy

Optimal control techniques are of great use in developing optimal strategies to control various kinds of malwares. In this work, to minimize the total density of infected nodes and the cost associated with the intervention measure, we use the optimal control theory [17].

For our purpose, let $[0,T]$ denote the time period during a control strategy that is imposed on system (2.1), and introduce a Lebesgue square integrable control function $u(t)$ $(0 \le t \le T)$, the budget for buying antivirus software at time t, which is

normalized to fall between 0 and 1 [29]. Then the admissible set of control function is given by

$$U=\{u(t)\in L^2[0.T]: 0\le u(t)\le 1, 0\le t\le T\}.$$

Therefore, system (2.1) can be transformed into the following control system:

$$\begin{cases}\dfrac{dS}{dt}=rS(1-\frac{S}{K})-\beta SI-\eta S+\delta R(t-\tau)+\gamma u(t)I,\\ \dfrac{dI}{dt}=\beta SI-\varepsilon I-\eta I-u(t)I,\\ \dfrac{dR}{dt}=\varepsilon I-\eta R-\delta R(t-\tau)+(1-\gamma)u(t)I,\end{cases}\tag{5.1}$$

with initial conditions

$$\begin{cases}S(t)=S_0\ge 0, & t\in[-\tau,0],\\ I(t)=I_0\ge 0, & t\in[-\tau,0],\\ R(t)=R_0\ge 0, & t\in[-\tau,0],\end{cases}\tag{5.2}$$

where γ denotes the control coefficient and $\gamma\in[0,1]$. Next, we shall try to find a control function $u(t)$ so that the functional

$$J(u)=\int_0^T\left[I(t)+\frac{\alpha u^2(t)}{2}\right]dt\tag{5.3}$$

is minimized, where α is s tradeoff factor. That is to minimize the total density of infected nodes and the cost associated with the intervention measure.

Lemma 6. *The system (5.1) with any initial conditions has a unique solution.*

Proof. We can rewrite (5.1) in the following form:

$$\frac{dV(t)}{dt}=AV(t)+BV_\tau(t)+F(V(t),u(t)),\tag{5.4}$$

where

$$V(t)=(S(t),I(t),R(t))^T,\quad V_\tau(t)=(S(t-\tau),I(t-\tau),R(t-\tau))^T,$$

$$A=\begin{pmatrix}r-\eta & 0 & 0\\ 0 & -\eta-\varepsilon & 0\\ 0 & \varepsilon & -\eta\end{pmatrix},\quad B=\begin{pmatrix}0 & 0 & \delta\\ 0 & 0 & 0\\ 0 & 0 & -\delta\end{pmatrix},$$

$$F=\begin{pmatrix}-\frac{r}{K}S^2(t)-\beta S(t)I(t)+\gamma u(t)I(t)\\ \beta S(t)I(t)-u(t)I(t)\\ (1-\gamma)u(t)I(t)\end{pmatrix}.$$

A simple calculation shows that

$$|F(V_1(t),u_1(t))-F(V_2(t),u_2(t))|\le M|V_1(t)-V_2(t)|,$$

where M is some positive constant, independent of state variables $S(t)$, $I(t)$ and $R(t)$. Furthermore, we have

$$|V_1(t)-V_2(t)|=|S_1(t)-S_2(t)|+|I_1(t)-I_2(t)|+|R_1(t)-R_2(t)|$$

and

$$|(V_1)_\tau(t)-(V_2)_\tau(t)|=|(S_1)_\tau(t)-(S_2)_\tau(t)|+|(I_1)_\tau(t)-(I_2)_\tau(t)|+|(R_1)_\tau(t)-(R_2)_\tau(t)|.$$

Therefore, it is easy to show that

$$AV(t)+BV_\tau(t)+F(V(t),u(t))\le L(|V_1(t)-V_2(t)|+|(V_1)_\tau(t)-(V_2)_\tau(t)|),\tag{5.5}$$

where $L=\max\{M,\|A\|,\|B\|\}<\infty$. Thus the terms on the right hand side of Eq. (5.4) are uniformly Lipschitz continuous. The solution of system (5.1) exists from (5.5) and taking into account the constraints on the controls $u(t)$ and the restrictions on the non-negativeness of the state variables.

In order to find an optimal solution, first we find the Lagrangian and Hamiltonian for the optimal control problem (5.1)–(5.3). Here the Lagrangian of the problem is

$$L(S,I,R,u)=I(t)+\frac{\alpha u^2(t)}{2}.$$

We seek the minimal value of the Lagrangian. To accomplish this, we define the Hamiltonian H for the control problem as

$$\begin{aligned}H(S,I,R,u,\lambda_1,\lambda_2,\lambda_3,t)&=L(S,I,R,u)+\lambda_1(t)\left\{rS\left(1-\frac{S}{K}\right)\right.\\&\left.-\beta SI-\eta S+\delta R(t-\tau)+\gamma u(t)I\right\}\\&+\lambda_2(t)\{\beta SI-\varepsilon I-\eta I-u(t)I\}\\&+\lambda_3(t)\{\varepsilon I-\eta R-\delta R(t-\tau)+(1-\gamma)u(t)I\},\end{aligned}\tag{5.6}$$

where $\lambda_1(t)$, $\lambda_2(t)$ and $\lambda_3(t)$ are the adjoint functions to be determined suitable. □

Lemma 7. *There exists an optimal control $u^*(t)$ such that $J(u^*(t))=\min_u J(u((t))$, subject to the control system (5.1) with initial conditions.*

Proof. In fact, the following conditions are satisfied:

1. The set of control and corresponding state variables is not empty.
2. The control space U is convex and closed by definition.
3. Each right hand side of the state system is continuous and is bounded by a sum of the bounded control and the state. Furthermore, it can be written as a linear function of the control variate $u(t)$ with coefficients depending on time and the state.
4. The integrand in the functional (5.3) is convex on the control set U and is bounded below.

Thus, according to Lukes [35], there exists an optimal control $u^*(t)$. This completes the proof. □

Next, let us derive a necessary condition for the optimal control strategy by means of the Pontryagin's Maximum Principle [24,25].

Theorem 4. *Let $S^\star(t)$, $I^\star(t)$, $R^\star(t)$ be optimal state solutions associated with the optimal control variable $u^*(t)$ for the optimal control problem (5.1)–(5.3). Then there exist adjoint variables $\lambda_1(t)$, $\lambda_2(t)$ and $\lambda_3(t)$ satisfying*

$$\frac{d\lambda_1(t)}{dt}=\lambda_1(t)\left[\frac{2r}{K}S^\star(t)+\beta I^\star(t)+\eta-r\right]-\lambda_2(t)\beta I^\star(t),\tag{5.7}$$

$$\begin{aligned}\frac{d\lambda_2(t)}{dt}&=\lambda_1(t)[\beta S^\star(t)-\gamma u^*(t)]+\lambda_2(t)[\varepsilon+\eta+u^*(t)-\beta S^\star(t)]\\&-\lambda_3(t)[\varepsilon+(1-\gamma)u^*(t)]-1,\end{aligned}\tag{5.8}$$

$$\frac{d\lambda_3(t)}{dt}=\lambda_3(t)+\chi_{[0,T-\tau]}\delta[\lambda_3(t+\tau)-\lambda_1(t+\tau)],\tag{5.9}$$

with transversality conditions

$$\lambda_i(T)=0,\quad i=1,2,3.$$

Furthermore, the optimal control is given as follows:

$$u^*(t)=\max\left\{\min\left\{[-\gamma\lambda_1(t)+\lambda_2(t)-(1-\gamma)\lambda_3(t)]\frac{I^\star(t)}{\alpha},1\right\},0\right\}.\tag{5.10}$$

Proof. To determine the adjoint equations and the transversality conditions we use the Hamiltonian (5.6). By using the necessary condition for optimal control problems which is found in [34], and

differentiating the Hamiltonian (5.6) with S, I, and R, we obtain

$$\frac{d\lambda_1(t)}{dt} = -H_S(t) - \chi_{[0,T-\tau]} H_{S_\tau}(t+\tau), \tag{5.11}$$

$$\frac{d\lambda_2(t)}{dt} = -H_I(t) - \chi_{[0,T-\tau]} H_{I_\tau}(t+\tau), \tag{5.12}$$

$$\frac{d\lambda_3(t)}{dt} = -H_R(t) - \chi_{[0,T-\tau]} H_{R_\tau}(t+\tau), \tag{5.13}$$

where H_x and H_{x_τ} denote the derivative with respect to x ($x = S, I, R$) and x_τ ($x_\tau = S(t-\tau), I(t-\tau), R(t-\tau)$), respectively. Thus, if we set $S(t) = S^\star(t)$, $I(t) = I^\star(t)$ and $R(t) = R^\star(t)$, then by substituting the corresponding derivatives in the above inequations and rearranging we obtain the adjoint equations (5.7)–(5.9). By using the optimality condition, we get

$$\left.\frac{\partial H}{\partial u}\right|_{u(t)=u^*(t)} = \alpha u^*(t) + \gamma\lambda_1(t) I^\star(t) - \lambda_2(t) I^\star(t) + (1-\gamma)\lambda_3(t) I^\star(t).$$

Considering the feature of the admissible set U, we have

$$u^*(t) = \max\left\{\min\left\{[-\gamma\lambda_1(t) + \lambda_2(t) - (1-\gamma)\lambda_3(t)]\frac{I^\star(t)}{\alpha}, 1\right\}, 0\right\}.$$

This completes the proof. □

Therefore, according to the analysis above, we can easily obtain the following optimality system:

$$\begin{cases} \dfrac{dS^\star}{dt} = rS^\star\left(1 - \dfrac{S^\star}{K}\right) - \beta S^\star I^\star - \eta S^\star + \delta R^\star(t-\tau) \\ \quad + \gamma \max\left\{\min\left\{[-\gamma\lambda_1(t) + \lambda_2(t) - (1-\gamma)\lambda_3(t)]\dfrac{I^\star}{\alpha}, 1\right\}, 0\right\} I^\star, \\ \dfrac{dI^\star}{dt} = \beta S^\star I^\star - \varepsilon I^\star - \eta I^\star \\ \quad - \max\left\{\min\left\{[-\gamma\lambda_1(t) + \lambda_2(t) - (1-\gamma)\lambda_3(t)]\dfrac{I^\star}{\alpha}, 1\right\}, 0\right\} I^\star, \\ \dfrac{dR^\star}{dt} = \varepsilon I^\star - \eta R^\star - \delta R^\star(t-\tau) + (1-\gamma) \\ \quad \max\left\{\min\left\{[-\gamma\lambda_1(t) + \lambda_2(t) - (1-\gamma)\lambda_3(t)]\dfrac{I^\star}{\alpha}, 1\right\}, 0\right\} I^\star, \\ S(t) = S_0 \geq 0, \quad I(t) = I_0 \geq 0, \quad R(t) = R_0 \geq 0, \quad t \in [-\tau, 0], \end{cases} \tag{5.14}$$

with the Hamiltonian H^* at $(S^\star, I^\star, R^\star, u^*, \lambda_1, \lambda_2, \lambda_3, t)$.

In order to ensure the correctness of the conclusion above, in next section, we will numerically solve the optimal control system (5.14) by using the Runge–Kutta fourth order scheme.

6. Numerical simulation and discussion

In this section, first we simulate and analyze the dynamic characteristics of the proposed SIRS malware propagation model without the optimal control strategy through Matlab, including the trend in the quantity of infected nodes. Furthermore, by using a Matlab code dde23 which is based on a standard Runge–Kutta scheme, we consider the optimal control problem (5.1) and verify the validity of our controller.

6.1. Impact of delays on the malware propagation model

To observe the impact of delays on the density of the infected nodes, we consider system (2.1) with $r=0.3$, $K=2$, $\beta=0.5$, $\varepsilon=0.4$, $\eta=0.1$, $\delta=0.2$. It is obvious that system (2.1) has a unique positive equilibrium point $E^* = (1, 0.2143, 0.2857)^T$. By calculating, the parameters satisfy the conditions of Theorem 2. According to Theorem 2, substituting these parameters into (3.8) yields two positive and simple roots, i.e., $\omega_1 = 0.2638$, $\omega_2 = 0.1860$. From (3.17) and (3.18), we can obtain the critical values of time delays τ as following:

$$\tau_{n,1} = 9.3646, 33.1809, 56.9973, 80.8136, \ldots,$$

$$\tau_{n,2} = 16.5713, 50.3499, 84.1285, 117.9071, \ldots.$$

These critical time delays can be ranked as

$$0 < \tau_{0,1} = 9.3646 < \tau_{0,2} = 16.5713 < \tau_{1,1} = 33.1809 < \tau_{1,2} = 50.3499$$

$$< \tau_{2,1} = 56.9973 < \tau_{3,1} = 80.8136 < \tau_{2,2} = 84.1285 < \tau_{3,2} = 117.9071 < \cdots.$$

Furthermore,

$$\left.\frac{d(\mathrm{Re}\ \lambda(\tau))}{d\tau}\right|_{\tau=\tau_{n,1}, \lambda=i\omega_1} = 0.0029 > 0 \quad \text{and}$$

$$\left.\frac{d(\mathrm{Re}\ \lambda(\tau))}{d\tau}\right|_{\tau=\tau_{n,2}, \lambda=i\omega_2} = -0.0011 < 0.$$

Thus, a pair of eigenvalues are crossing the imaginary axis from the left to the right when $\tau = \tau_{n,1}$ and from the right to the left when $\tau = \tau_{n,2}$. The time histories for the delay chosen from different regions are shown in Figs. 2–7. The positive equilibrium point E^* of system (2.1) is locally asymptotically stable when $\tau \in [0, \tau_{0,1}) \cup (\tau_{0,2}, \tau_{1,1}) \cup (\tau_{2,2}, \tau_{2,1})$, and it loses its stability for $\tau \in (\tau_{0,1}, \tau_{0,2}) \cup (\tau_{1,1}, \tau_{1,2}) \cup (\tau_{2,1}, \infty)$. In a word, time delay leads system (2.1) to exhibit the multiple switches phenomenon of rest state from stable to unstable, then back to stable. The positive equilibrium point E^* of system (2.1) is unstable in the end.

On the other hand, when $\tau = \tau_{0,1} = 9.3646$ we can compute $c_1(0) = 1.7083 - 2.7922i$, $\sigma_2 = -(1.7083/\mathrm{Re}(\lambda'(\tau_{0,1}))) = -594.4211 < 0$, $\beta_2 = 2\,\mathrm{Re}(c_1(0)) = 3.4167 > 0$. Therefore, from the discussions in Section 4, we know that the bifurcated periodic solutions

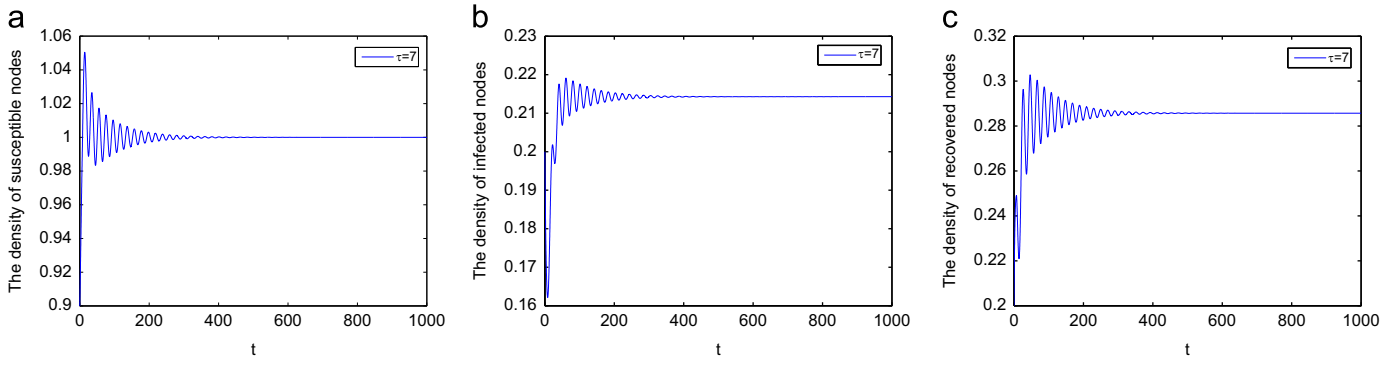

Fig. 2. The positive equilibrium point E^* is locally asymptotically stable when $\tau = 7 \in [0, \tau_{0,1})$.

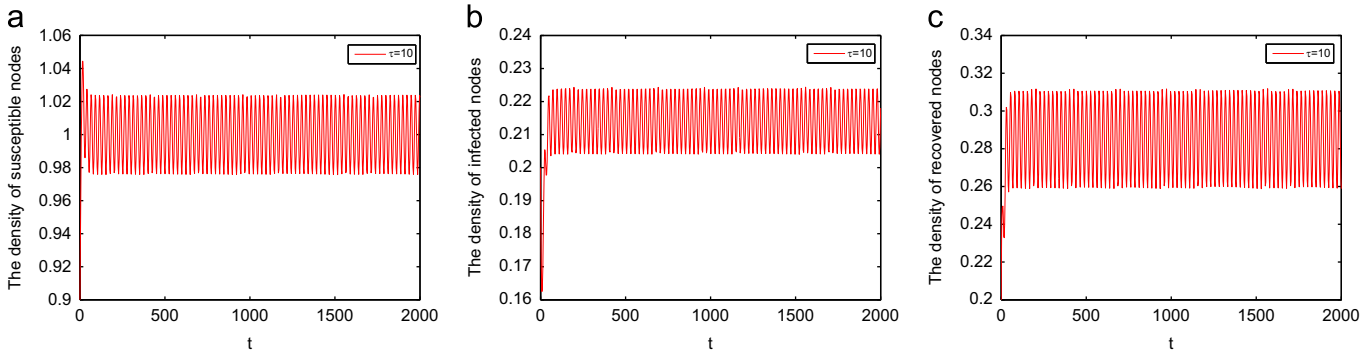

Fig. 3. The periodic oscillation derived from Hopf bifurcation around the positive equilibrium point E^* occurs when $\tau = 10 \in (\tau_{0,1}, \tau_{0,2})$.

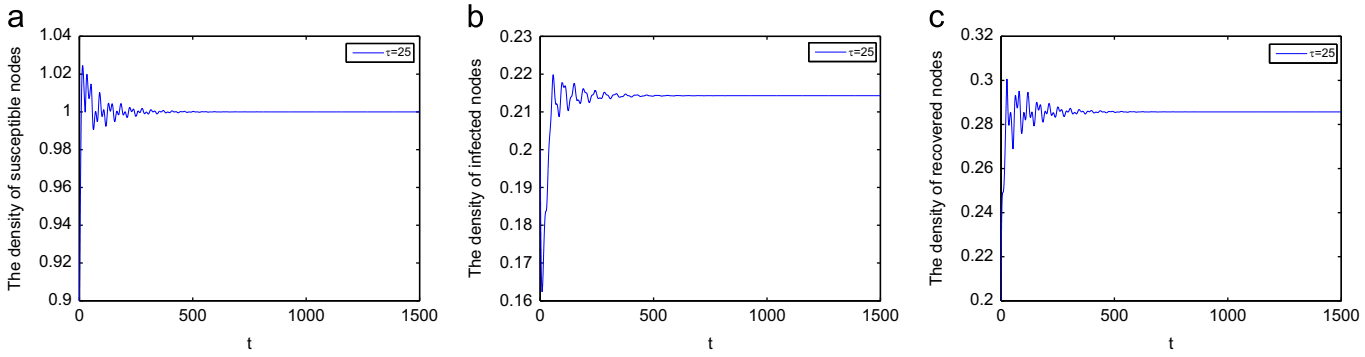

Fig. 4. The positive equilibrium point E^* is locally asymptotically stable when $\tau = 25 \in (\tau_{0,2}, \tau_{1,1})$.

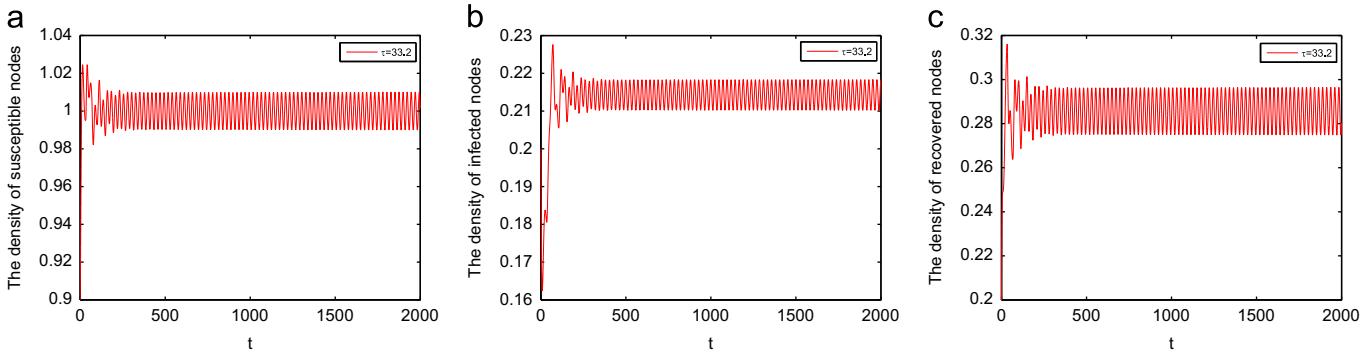

Fig. 5. The periodic oscillation derived from Hopf bifurcation around the positive equilibrium point E^* occurs when $\tau = 33.2 \in (\tau_{1,1}, \tau_{1,2})$.

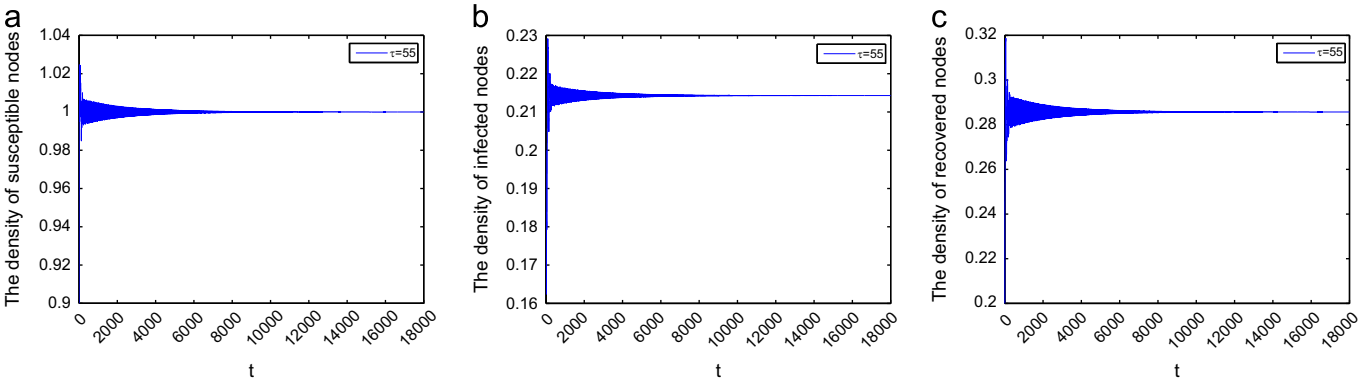

Fig. 6. The positive equilibrium point E^* is locally asymptotically stable when $\tau = 55 \in (\tau_{1,2}, \tau_{2,1})$.

are orbitally unstable on the center manifold. In addition, from Theorem 3, we know that system (2.1) has an unstable center manifold near the positive equilibrium point E^* for τ near $\tau_{0,1}$. Therefore, the bifurcating periodic solution of system (2.1) is unstable on the center manifold and the Hopf bifurcation is subcritical. We cannot get the bifurcating periodic solutions from simulations [36]. Similarly, for the other critical values of

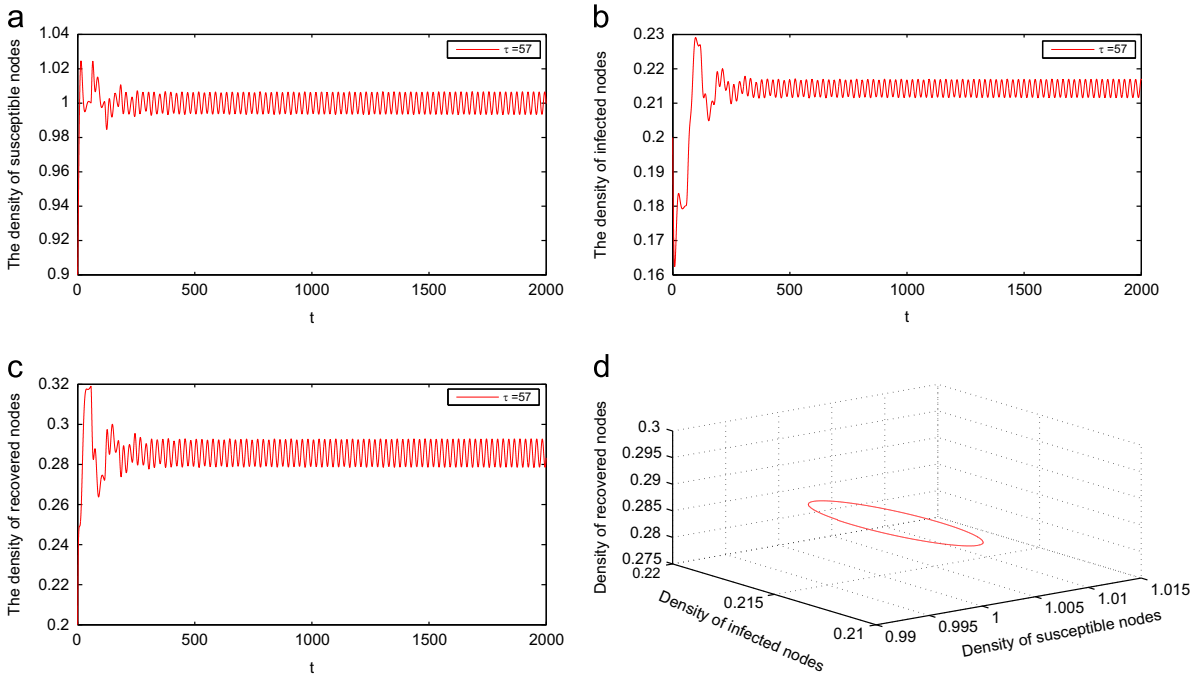

Fig. 7. The periodic oscillation derived from Hopf bifurcation around the positive equilibrium point E^* occurs when $\tau = 57 \in (\tau_{2,1}, \tau_{3,1})$.

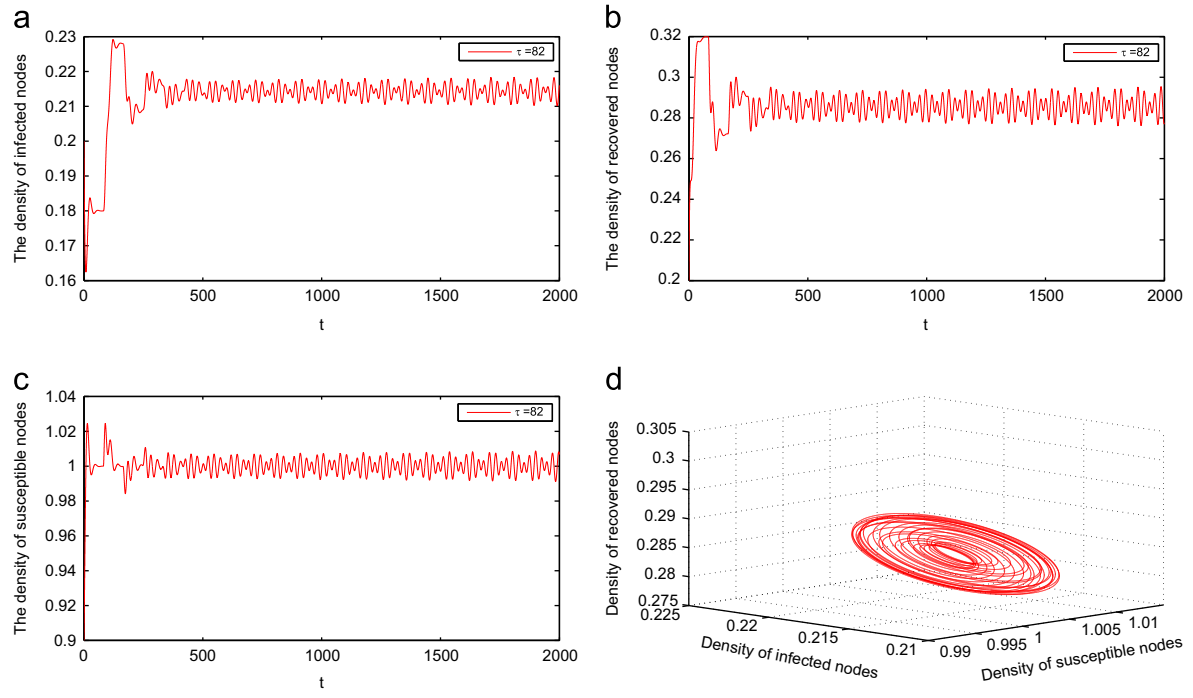

Fig. 8. The attractive quasi-periodic oscillation derived from Hopf bifurcation around the positive equilibrium point E^* occurs when $\tau = 82 \in (\tau_{3,1}, \tau_{2,2})$.

time delay τ we can also analyze their direction and stability of bifurcating periodic oscillations.

Furthermore, we choose $\tau = 82$. According to Theorem 2, a periodic oscillation derived from Hopf bifurcation around the positive equilibrium point E^* occurs, as shown in Fig. 8. From Fig. 8, we can see that system (2.1) has an attractive quasi-periodic solution, which is different from the discussion above (such as Fig. 7). This means that malware propagation is sensitive to the immune period τ of a recovered node. The above observations provide new insights into the malware propagation in WSNs that the impact of delays on the malware propagation model cannot be ignored, namely, with the delay τ increasing the wireless sensor networks lose stability through a Hopf bifurcation and some oscillations occur, then come back to a stable state again, and in the end it becomes unstable. The phenomenon possibly leads to that the utilization of the network decreases and the network performance declines.

6.2. *Impact of optimal control strategy on the malware propagation model*

In this part, we will numerically illustrate that the optimal control strategy we proposed can effectively extend the region of stability of system (2.1) and also decrease the density of infected nodes in WSNs.

Example 1 (*Impact of optimal control strategy on the region of stability*). Consider system (5.1) with $r=0.7$, $K=2$, $\beta=0.3$, $\varepsilon=0.3$, $\eta=0.05$, $\delta=0.4$, $\alpha=6$ and $\gamma=0.3$. It is easy to obtain that the positive equilibrium point of uncontrolled system (2.1) is $E^*=(1.1667, 3.3833, 2.2556)^T$ and the critical value of delay is $\tau_0=6.8345$. Without loss of generality, we assign $\tau=4,5,6<\tau_0$ with the other parameters unchanged. The simulation results are shown in Fig. 9(a). From Fig. 9(a), we notice that the density of infected nodes converges to the positive equilibrium point E^* of system (2.1). Thus the malware continuously propagates in WSNs. In addition, from Fig. 9(a) we notice that a larger τ implies a longer convergence time. For optimal control system (5.1) we also choose $\tau=4,5,6$. As shown in Fig. 9(b), we can see that system (5.1) quickly converges to the positive equilibrium point and it is independent on delay. Thus, the optimal control strategy is more effective to guarantee the system to work normally.

Furthermore, we set $\tau=6.84, 7.24, 7.94$. According to Theorem 1, the periodic oscillation derived from Hopf bifurcation around the positive equilibrium point E^* occurs, as shown in Figs. 10(a), 11(a) and 12(a). In addition, with τ increasing we find that the amplitude of uncontrolled system (2.1) increases, which possibly leads to that the utilization of the network decreases and the network performance declines. For the optimal control system (5.1), it is easy to show that system (5.1) is asymptotically stability and the density of infected nodes is lower than the uncontrolled system (2.1), as shown in Figs. 10(b), 11(b) and 12(b). Thus, the optimal control strategy effectively extends the region of stability of system (2.1).

Example 2 (*Impact of optimal control strategy on the density of different nodes*). In this part, we have plotted susceptible nodes, infected nodes and recovered nodes with and without control by considering values of parameters as $r=0.7$, $K=6$, $\beta=0.5$, $\varepsilon=0.3$,

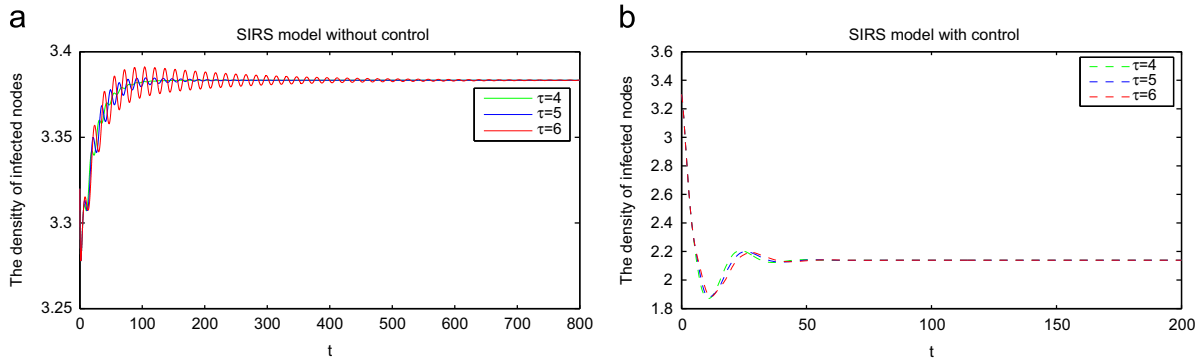

Fig. 9. Uncontrolled system (2.1) and optimal control system (5.1) are asymptotically stable when $\tau=4,5,6$.

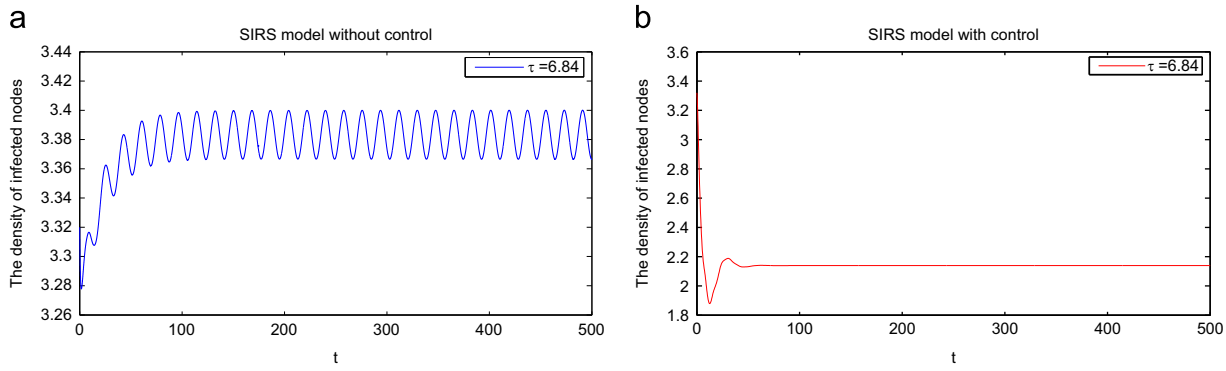

Fig. 10. (a) The periodic oscillation derived from Hopf bifurcation around the positive equilibrium point E^* occurs when $\tau=6.84>\tau_0$. (b) Optimal control system (5.1) is asymptotically stable when $\tau=6.84$.

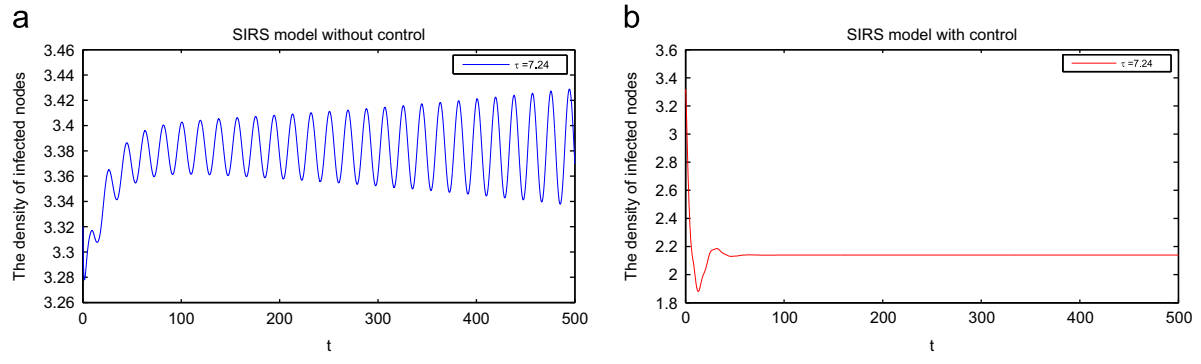

Fig. 11. (a) The periodic oscillation derived from Hopf bifurcation around the positive equilibrium point E^* occurs when $\tau=7.24>\tau_0$. (b) Optimal control system (5.1) is asymptotically stable when $\tau=7.24$.

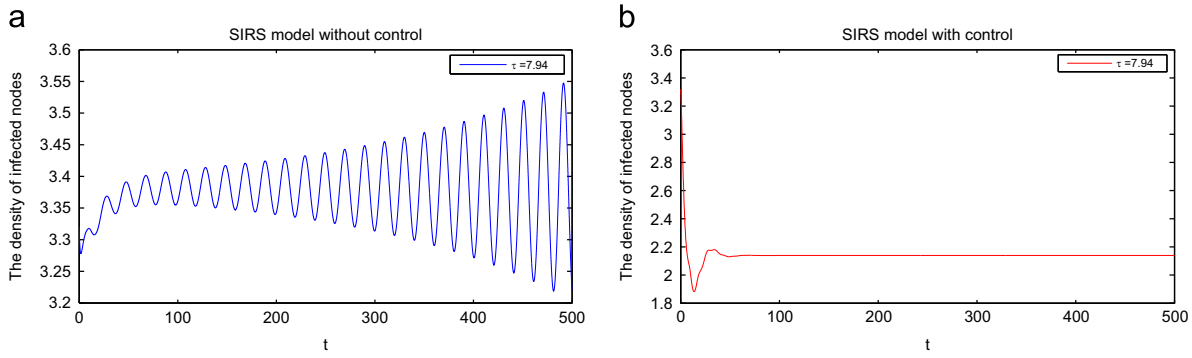

Fig. 12. (a) The periodic oscillation derived from Hopf bifurcation around the positive equilibrium point E^* occurs when $\tau = 7.94 > \tau_0$. (b) Optimal control system (5.1) is asymptotically stable when $\tau = 7.94$.

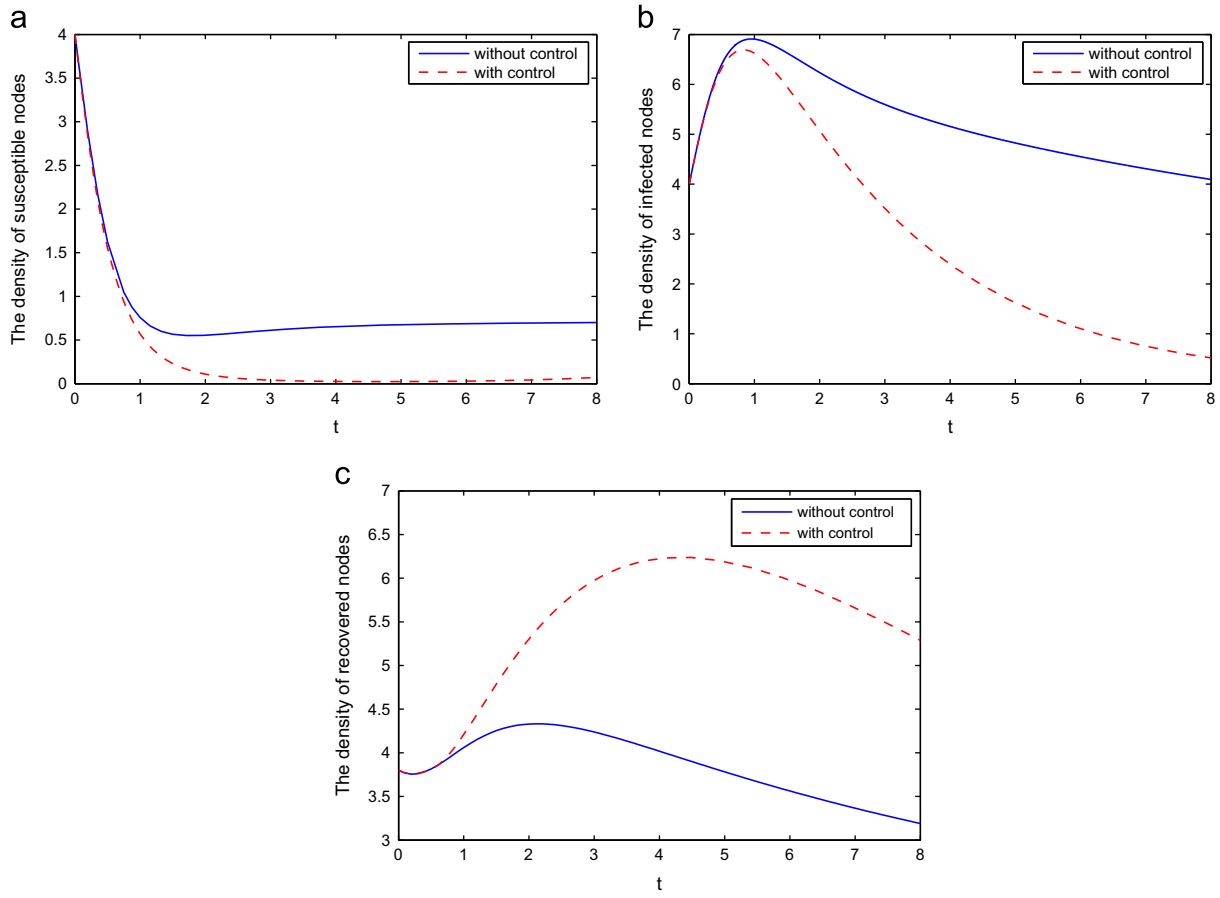

Fig. 13. The plots represent the density of nodes in three different states both with control and without control. (a) Susceptible nodes. (b) Infected nodes. (c) Recovered nodes. (For interpretation of the references to color in this figure caption, the reader is referred to the web version of this article.)

Table 1
The dynamic behavior of system (2.1) for different constant rate δ.

δ	Positive equilibrium point	Stability domain	σ_2	β_2	T_2
0.35	$(0.8250, 0.6277, 0.3649)^T$	[0, 4.4388)	−67.8808	3.5794	−5.5097
0.40	$(0.8250, 0.6527, 0.3399)^T$	[0, 3.8609)	442.4170	−33.4101	43.1185
0.45	$(0.8250, 0.6744, 0.3181)^T$	[0, 3.4224)	15.3341	−1.5498	1.8049

$\eta = 0.1$, $\delta = 0.3$, $\alpha = 6$, $\gamma = 0.6$ and $\tau = 0.5$. The control nodes are marked by red dashed line while the nodes without control are marked by blue solid line.

In Fig. 13(a), we have plotted susceptible nodes with and without control. The numerical results show that the density of susceptible nodes quickly decreases and goes to a stable state. In addition, we can

see that the density of infected nodes in the optimal control system (5.1) is smaller than that in the uncontrolled system (2.1).

Fig. 13(b) represents the density of infected nodes in the two systems (2.1) without control and (5.1) with control. Obviously, the density of infected nodes without control is larger than the density of infected nodes with optimal control strategy, so we need treatment to control the infected nodes.

In Fig. 13(c), we obtain that the density of recovered nodes in the optimal control system (5.1) is larger, which is more effective to guarantee the system to work normally.

7. Discussion and concluding remarks

In this paper, we have developed a SIRS model for malware propagation in WSNs, and have discussed the stability and Hopf bifurcation. Considering the discrete delay τ as bifurcation parameter, the existence, stability, and direction of bifurcation periodic solutions are investigated in detail by applying the theorem of partial function differential equation, the normal form method and center manifold theorem. In order to minimize the density of infected nodes and the cost associated with the intervention measure, we propose a optimal control strategy (see the optimal control system (5.1)). Numerical simulations reveal that the discrete delay is responsible for the stability switches of the model system, and a Hopf bifurcation occurs as the delay increasing through a certain threshold. In addition, we obtain that the optimal control strategy effectively extends the region of stability and minimizes the density of infected nodes. Thus, the SIRS malware propagation model with a optimal control strategy provides new insights into the malware propagation in WSNs.

In order to reduce the density of infected nodes and guarantee system (2.1) to work normally, we must pay more addition to the factor of δ (the rate constant for nodes becoming susceptible again after recovered). In fact, the dependence of the density I^* of infected nodes on the contact rate (the parameter δ) may be found by observing that

$$\frac{dI^*}{d\delta}=\frac{\varepsilon(\eta+\varepsilon)[r(K\beta-\varepsilon-\eta)-K\beta\eta]}{K\eta\beta^2(\varepsilon+\eta+\delta)^2}>0$$

under the condition (H_2), so that I^* is an increasing function about δ. In this section, we will further discuss the effect of δ on the density of infected nodes and the dynamic characteristic of system (2.1).

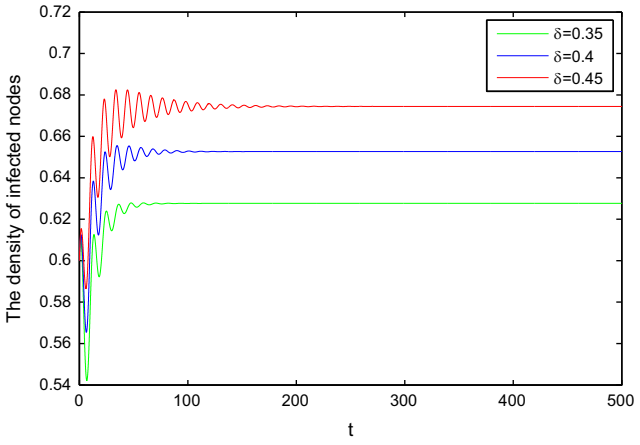

Fig. 14. The positive equilibrium point E^* is locally asymptotically stable with δ increasing when $\tau=3<\tau_0$.

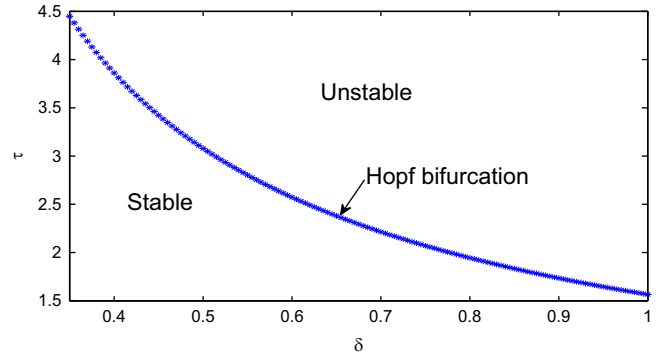

Fig. 16. The region of stability of system (2.1) varies with the constant rate δ increasing.

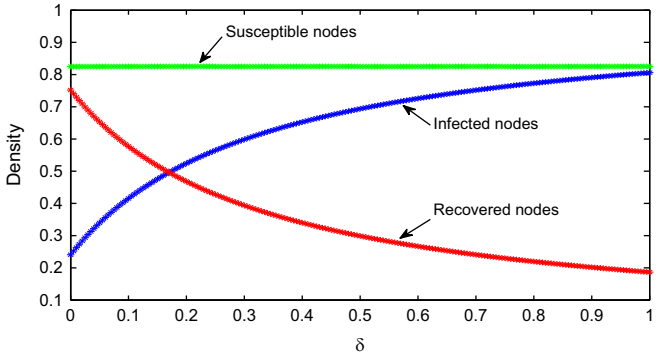

Fig. 17. The positive equilibrium points of system (2.1) varies with the constant rate δ increasing.

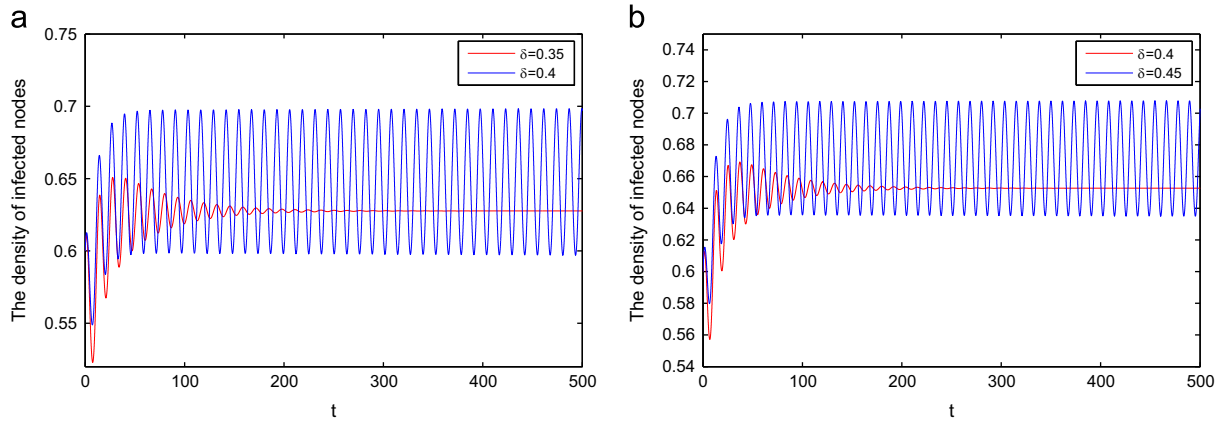

Fig. 15. (a) The dynamic characteristic of system (2.1) with different δ and time delay τ. (a) Set $\tau=3.87$, and $\delta=0.35, 0.4$. (b) Set $\tau=3.43$, and $\delta=0.4, 0.45$.

Consider system (2.1) with $r=0.3$, $K=2$, $\beta=0.4$, $\varepsilon=0.25$, $\eta=0.08$ and assign 0.35, 0.40 and 0.45 to δ, respectively. Obviously, the conditions (H_2)–(H_4) hold. According to Theorems 1 and 3, by calculating, it is easy to obtain the corresponding positive equilibrium points and the dynamic behavior of system (2.1) for different δ, as shown in Table 1.

From Table 1, we can obtain that with the increasing of δ, the critical value of τ decreases. This means that the region of stability of system (2.1) decreases and the malware propagation is sensitive to δ. Moveover, if $\delta=0.40$ or $\delta=0.45$, then when $\tau=\tau_0$, we have $\sigma_2>0$, $\beta_2<0$. Therefore, from the discussions in Section 4, we know that the bifurcating periodic solutions are orbitally asymptotically stable on the center manifold. In addition, from Theorem 3, we know that system (2.1) has a stable center manifold near the positive equilibrium point E^* for τ near τ_0. Thus, the center manifold theory implies that the bifurcated periodic solutions of system (2.1) when $\tau=\tau_0$ in the whole phase space are orbitally asymptotically stable, and the Hopf bifurcation is supercritical for $\sigma_2>0$. When $\delta=0.35$, we have $\sigma_2<0$, $\beta_2>0$. Therefore, from the discussions in Section 4, we know that the bifurcating periodic solutions are orbitally unstable on the center manifold. In addition, we have that in the whole phase space the Hopf bifurcation is subcritical.

Without loss of generality, we assign $\tau=3<\tau_0$ with the other parameters unchanged. The simulation results are shown in Fig. 14. From Fig. 14, we notice that the density of infected nodes converges to the positive equilibrium point E^* of system (2.1). Thus at last the malware continuously propagates in WSNs. The simulation results in Fig. 14 verify Theorem 1. In addition, from Fig. 14 we notice that with the increasing of δ, the convergence time becomes longer and at last the density of infected nodes increases. Furthermore, form Fig. 15 we can see that with the increasing of the constant rate δ the region of system (2.1) decreases. This means that the dynamic behave is sensitive to δ. Thus, if we want to guarantee the system to work normally, we must strengthen prevention measures to the wireless sensor networks.

Remark 1. Keep the parameters $r=0.3$, $K=2$, $\beta=0.4$, $\varepsilon=0.25$, $\eta=0.08$. In this part, we discuss the effect of δ on the region of stability of system (2.1) when δ varies from 0.3 to 1 continuously, as shown in Fig. 16. From Fig. 16, we can see that with δ increasing, the region of system (2.1) decreases quickly, which implies that WSNs possibly decrease the utilization and decline the performance when δ increases. The above observations provide new insight into the malware propagation in WSNs.

Remark 2. Keep the parameters $r=0.3$, $K=2$, $\beta=0.4$, $\varepsilon=0.25$, $\eta=0.08$, but δ varies in $[0,1]$, the corresponding situations of positive equilibrium points are shown in Fig. 17. Fig. 17 shows that with the increase of the constant rate δ, the density of the susceptible nodes and the recovered nodes is decreasing and the density of the infected nodes is increasing. Obviously, the increasing of δ is harmful for the wireless sensor networks. Thus, we must take the necessary measures to decrease δ, such as enhance the strength of the antivirus software.

Acknowledgments

This research is supported by National Natural Science Foundation of China under Grants 61174155 and 11032009. The work is also sponsored by Qing Lan Project to Jiangsu.

References

[1] P.K. Sahoo, J.-P. Sheu, K.-Y. Hsieh, Target tracking and boundary node selection algorithms of wireless sensor networks for internet services, Inf. Sci. 230 (2013) 21–38.
[2] I. Khemapech, Feasibility study of direct communication in wireless sensor networks, Proc. Comput. Sci. 21 (2013) 424–429.
[3] Q. Ren, Q. Liang, Energy and quality aware query processing in wireless sensor database systems, Inf. Sci. 177 (2007) 2188–2205.
[4] F. Guerriero, A. Violi, E. Natalizio, V. Loscri, C. Costanzo, Modelling and solving optimal placement problems in wireless sensor networks, Appl. Math. Model. 35 (1) (2011) 230–241.
[5] S.S. Lee, P.-K. Tseng, A. Chen, Link weight assignment and loop-free routing table update for link state routing protocols in energy-aware internet, Future Gener. Comput. Syst. 28 (2) (2012) 437–445.
[6] T. Rault, A. Bouabdallah, Y. Challal, Energy efficiency in wireless sensor networks: a top-down survey, Comput. Netw. 67 (2014) 104–122.
[7] W. Xu, J. Cao, M. Xiao, Bifurcation analysis and control in exponential RED algorithm, Neurocomputing 129 (2014) 232–245.
[8] T. Dong, X. Liao, HopfČPitchfork bifurcation in a simplified BAM neural network model with multiple delays, J. Comput. Appl. Math. 253 (1) (2013) 222–234.
[9] Z. Cheng, J. Cao, Hybrid control of Hopf bifurcation in complex networks with delays, Neurocomputing 131 (2014) 164–170.
[10] B.K. Mishra, N. Keshri, Mathematical model on the transmission of worms in wireless sensor network, Appl. Math. Model. 37 (6) (2013) 4103–4111.
[11] P. De, Y. Liu, S.K. Das, An epidemic theoretic framework for vulnerability analysis of broadcast protocols in wireless sensor networks, IEEE Trans. Mob. Comput. 8 (3) (2009) 413–425.
[12] S. Zanero, Wireless malware propagation: a reality check, IEEE Trans. Secur. Priv. 7 (5) (2009) 70–74.
[13] M.E. Newman, Spread of epidemic disease on networks, Phys. Rev. E 66 (2002) 016128.
[14] Z. Chen, C. Ji, Spatial-temporal modeling of malware propagation in networks, IEEE Trans. Neural Netw. 16 (5) (2005) 1291–1303.
[15] X. Wang, Q. Li, Y. Li, Eisirs: a formal model to analyze the dynamics of worm propagation in wireless sensor networks, J. Comb. Optim. 20 (2010) 47–62.
[16] X. Wang, Y. Li, An improved sir model for analyzing the dynamics of worm propagation in wireless sensor networks, Chin. J. Electron. 18 (2009) 8–12.
[17] A. Halanay, Optimal controls for systems with time lag, SIAM J. Control 6 (2) (1968) 215–234.
[18] C. Liu, Z. Gong, B. Shen, E. Feng, Modelling and optimal control for a fed-batch fermentation process, Appl. Math. Model. 37 (3) (2013) 695–706.
[19] T. Kar, A. Batabyal, Stability analysis and optimal control of an sir epidemic model with vaccination, Biosystems 104 (2) (2011) 127–135.
[20] M. Goble, M.D. Iseman, L.A. Madsen, D. Waite, L. Ackerson, C.R. Horsburgh Jr., Treatment of 171 patients with pulmonary tuberculosis resistant to isoniazid and rifampin, N. Engl. J. Med. 328 (8) (1993) 527–532.
[21] C. Liu, Optimal control for nonlinear dynamical system of microbial fed-batch culture, J. Comput. Appl. Math. 232 (2) (2009) 252–261.
[22] A. Gumel, S. Moghadas, A qualitative study of a vaccination model with non-linear incidence, Appl. Math. Comput. 143 (2) (2003) 409–419.
[23] G.W. Swan, Role of optimal control theory in cancer chemotherapy, Math. Biosci. 101 (2) (1990) 237–284.
[24] S. Lenhart, J.T. Workman, Optimal Control Applied to Biological Models, CRC Press, London, 2007.
[25] M.I. Kamien, N.L. Schwartz, Dynamic Optimization: The Calculus of Variations and Optimal Control in Economics and Management, 1981.
[26] L. Feng, X. Liao, Q. Han, H. Li, Dynamical analysis and control strategies on malware propagation model, Appl. Math. Model. 37 (16) (2013) 8225–8236.
[27] T. Zhang, J. Liu, Z. Teng, Dynamic behavior for a nonautonomous SIRS epidemic model with distributed delays, Appl. Math. Comput. 214 (2) (2009) 624–631.
[28] Y. Lu, G. Jiang, Backward bifurcation and local dynamics of epidemic model on adaptive networks with treatment, Neurocomputing 145 (2014) 113–121.
[29] Q. Zhu, X. Yang, L. Yang, C. Zhang, Optimal control of computer virus under a delayed model, Appl. Math. Comput. 218 (2012) 1613–1619.
[30] Y. Song, J. Wei, Bifurcation analysis for Chen's system with delayed feedback and its application to control of chaos, Chaos, Solitons Fractals 22 (1) (2004) 75–91.
[31] A.A. Albert, An inductive proof of descartes' rule of signs, Am. Math. Mon. (1943) 178–180.
[32] J. Wu, Theory and Applications of Partial Functional Differential Equations, vol. 119, Springer, New York, 1996.
[33] J.K. Hale, Functional Differential Equations, Springer, New York, 1971.
[34] L. Göllmann, D. Kern, H. Maurer, Optimal control problems with delays in state and control variables subject to mixed control-state constraints, Optim. Contr. Appl. Met. 30 (2009) 341–365.
[35] D.L. Lukes, Differential Equations: Classical to Controlled, Academic Press, New York, 1982.
[36] W. Zuo, J. Wei, Stability and hopf bifurcation in a diffusive predator–prey system with delay effect, Nonlinear Anal.: Real World Appl. 12 (2011) 1998–2011.
[37] H. Hu, L. Huang, Stability and Hopf bifurcation analysis on a ring of four neurons with delays, Appl. Math. Comput. 213 (2009) 587–599.

Linhe Zhu received his B.S. degree in Applied Mathematics from Xinzhou Teachers University, Xinzhou, China. Now he is studying for a Ph.D. degree in Applied Mathematics at the Department of Mathematics, Nanjing University of Aeronautics and Astronautics, Jiangsu province, China. His research interests include dynamical system, neural networks, information sciences and control theory.

Hongyong Zhao received the Ph.D. degree from Sichuan University, Chengdu, China, and the Post-Doctoral Fellow in the Department of Mathematics at Nanjing University, Nanjing, China.

He was with the Department of Mathematics at Nanjing University of Aeronautics and Astronautics, Nanjing, China. He is currently a Professor of Nanjing University of Aeronautics and Astronautics, Nanjing, China. He is also the author or coauthor of more than 60 journal papers. His research interests include nonlinear dynamic systems, neural networks, control theory, and applied mathematics.